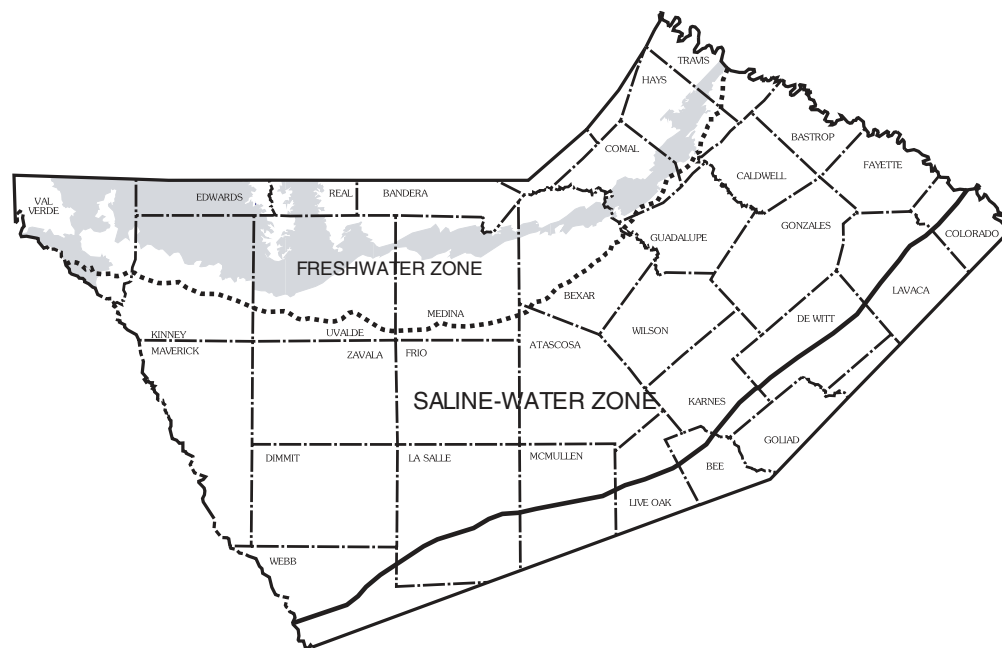


HYDROGEOLOGIC FRAMEWORK AND GEOCHEMISTRY OF THE EDWARDS AQUIFER SALINE-WATER ZONE, SOUTH-CENTRAL TEXAS

U.S. GEOLOGICAL SURVEY
Water-Resources Investigations Report 97-4133



*Prepared in cooperation with the
EDWARDS AQUIFER AUTHORITY and
SAN ANTONIO WATER SYSTEM*



**HYDROGEOLOGIC FRAMEWORK AND
GEOCHEMISTRY OF THE EDWARDS
AQUIFER SALINE-WATER ZONE,
SOUTH-CENTRAL TEXAS**

By George E. Groschen and Paul M. Buszka

**U.S. GEOLOGICAL SURVEY
Water-Resources Investigations Report 97-4133**



**Prepared in cooperation with the
EDWARDS AQUIFER AUTHORITY and
SAN ANTONIO WATER SYSTEM**

**Austin, Texas
1997**

U.S. DEPARTMENT OF THE INTERIOR

BRUCE BABBITT, Secretary

U.S. GEOLOGICAL SURVEY

Gordon P. Eaton, Acting Director

Any use of trade, product, or firm names is for descriptive purposes only and does not imply endorsement by the U.S. Government.

For additional information write to:

District Chief
U.S. Geological Survey
8011 Cameron Rd.
Austin, TX 78754-3898

Copies of this report can be purchased from:

U.S. Geological Survey
Branch of Information Services
Box 25286
Denver, CO 80225-0286

CONTENTS

Abstract	1
Introduction	1
Purpose and Scope	3
Methods of Data Collection and Analysis	3
Sampling Methods	3
Sample Preparation and Laboratory Analyses	4
Well-Numbering System	6
Acknowledgments	6
Hydrogeologic Framework	6
Geology and Stratigraphy of Aquifer Units	6
Kainer, Person, and Georgetown Formations	6
Devils River Formation	10
West Nueces, McKnight, and Salmon Peak Formations	10
Stuart City Formation	10
Stratigraphy of Underlying and Overlying Units	10
Glen Rose Limestone	10
Del Rio Clay, Buda Limestone, and Eagle Ford Group	10
Geologic Structure and Faults	11
Hydrologic Framework	11
Geochemistry of the Saline-Water Zone	13
Equilibrium Species Distribution	13
Application of Equilibrium-Computation Program	13
Uncertainties in Equilibrium Species Distribution	19
Temperature and Hydrogen Activity	19
Dissolved Constituents	21
Dissolved Solids	21
Chloride	24
Calcium and Magnesium	25
Sulfur	27
Dissolved, Gas Phase, and Nonaqueous Liquid Phase	27
Stable Isotopes	28
Carbon	31
Dissolved	31
Stable Isotopes	33
Other Dissolved Species	34
Other Isotopes	36
Stable Isotopes of Hydrogen and Oxygen	36
Stable Isotopes of Strontium and Boron	37
Unstable Isotopes of Carbon and Chloride	41
Summary and Conclusions	43
References	44

FIGURES

1. Map showing location of the study area	2
2. Diagram showing well-numbering system	7
3. Chart showing correlation of Cretaceous stratigraphic units in south Texas and Edwards aquifer hydrostratigraphic units in the San Marcos platform area, south-central Texas	8

4.	Map showing location of selected faults, oil and gas fields, and depositional provinces near the Edwards aquifer saline-water zone, south-central Texas	9
5.	Generalized hydrogeologic section showing the relation between the Edwards aquifer and the geopressured zone in the subsurface of the Texas Gulf Coast	12
6–7.	Maps showing:	
6.	Location of wells in the Edwards aquifer saline-water zone, south-central Texas, for which water-sample analyses are available	14
7.	Location of sampled wells and monitor-well transects in San Antonio, New Braunfels, and San Marcos, Texas	15
8–10.	Graphs showing:	
8.	Relation between estimated in-place temperature of ground-water samples and distance of well from the downdip limit of freshwater in the Edwards aquifer, south-central Texas	20
9.	Relation between corrected pH and dissolved solids concentration in ground-water samples from the Edwards aquifer saline-water zone, south-central Texas	20
10.	Relation between dissolved solids concentration in ground-water samples from the saline-water zone and distance of the well from the downdip limit of freshwater in the Edwards aquifer, south-central Texas	24
11.	Map showing mineral-saturation indices of dolomite and magnesite in ground-water samples from the Edwards aquifer saline-water zone, south-central Texas	26
12.	Graphs showing relations between (A) del sulfur-34 ($\delta^{34}\text{S}$) of dissolved sulfate and dissolved solids concentration, (B) $\delta^{34}\text{S}$ of dissolved sulfide and dissolved solids concentration, and (C) $\delta^{34}\text{S}$ of dissolved sulfate minus $\delta^{34}\text{S}$ of dissolved sulfide and estimated temperature in ground-water samples from the Edwards aquifer saline-water zone, south-central Texas	29
13.	Map showing distribution of del carbon-13 ($\delta^{13}\text{C}$) of dissolved inorganic carbon and del sulfur-34 ($\delta^{34}\text{S}$) of dissolved sulfate and sulfide in ground-water samples, and location of wells that produce water with meteoric del deuterium (δD) and del oxygen-18 ($\delta^{18}\text{O}$) in the Edwards aquifer saline-water zone, south-central Texas	30
14–20.	Graphs showing:	
14.	Relation between dissolved iron and dissolved solids concentrations in ground-water samples from the Edwards aquifer saline-water zone, south-central Texas	35
15.	Relation between dissolved potassium and dissolved solids concentrations in ground-water samples from the Edwards aquifer saline-water zone, south-central Texas	36
16.	Relation between del deuterium (δD) and del oxygen-18 ($\delta^{18}\text{O}$) in ground-water samples from the Edwards aquifer saline-water-zone, south-central Texas	37
17.	Relation between ratio of strontium-87/strontium-86 ($^{87}\text{Sr}/^{86}\text{Sr}$) of dissolved strontium and dissolved strontium concentration in ground-water samples from the Edwards aquifer saline-water zone, south-central Texas	39
18.	Ranges of del boron-11 ($\delta^{11}\text{B}$) of dissolved boron in selected natural materials and in water	40
19.	Relation between del boron-11 ($\delta^{11}\text{B}$) of dissolved boron and dissolved solids concentration in ground-water samples from the Edwards aquifer saline-water zone, south-central Texas	40
20.	Relations between (A) ratio of chlorine-36/chlorine ($^{36}\text{Cl}/\text{Cl}$) of dissolved chloride and ^{36}Cl , and (B) dissolved solids concentration and ^{36}Cl in ground-water samples from the Edwards aquifer saline-water zone, south-central Texas	42

TABLES

1.	Selected physical properties for samples from wells in the Edwards aquifer saline-water zone, south-central Texas, July–September 1990	16
2.	Alkalinity and concentrations of major dissolved ions and dissolved silica for samples from wells in the Edwards aquifer saline-water zone, south-central Texas, July–September 1990	17

3. Summary of mineral saturation indices computed by SOLMINEQ.88 (Kharaka and others, 1988) for samples from wells in the Edwards aquifer saline-water zone, south-central Texas, July–September 1990	18
4. Dissolved solids concentrations and anhydrous weight percentages of computed salt-normative mineral assemblages for samples from selected wells in the Edwards aquifer saline-water zone, south-central Texas, collected over various time periods	22
5. Concentrations of dissolved organic and inorganic carbon, dissolved bicarbonate, del carbon-13 ($\delta^{13}\text{C}$) of dissolved inorganic carbon, carbon-14 (^{14}C), and dissolved aliphatic acids for samples from wells in the Edwards aquifer saline-water zone, south-central Texas, July–September 1990	32
6. Concentrations of selected dissolved gases for samples from wells in the Edwards aquifer saline-water zone, south-central Texas, July–September 1990	33
7. Concentrations of minor dissolved ions for samples from wells in the Edwards aquifer saline-water zone, south-central Texas, July–September 1990	34
8. Stable-isotope ratios of selected dissolved species for samples from wells in the Edwards aquifer saline-water zone, south-central Texas, July–September 1990	38
9. Ratio of chlorine-36 to chlorine ($^{36}\text{Cl}/\text{Cl}$), number of ^{36}Cl atoms per liter, and associated error for samples from wells in the Edwards aquifer saline-water zone, south-central Texas, July–September 1990	43

VERTICAL DATUM AND ABBREVIATIONS

Sea level: In this report, "sea level" refers to the National Geodetic Vertical Datum of 1929—a geodetic datum derived from a general adjustment of the first-order level nets of both the United States and Canada, formerly called Sea Level Datum of 1929.

Per mil: A unit expressing the ratio of stable-isotope abundances of an element in a sample to those of a standard material. Per mil units are equivalent to parts per thousand. Stable-isotope ratios are calculated as follows:

$$\delta X = \left(\frac{R(\text{sample})}{R(\text{standard})} - 1 \right) \times 1,000 ,$$

where X is the heavier isotope, and

R is the ratio of the heavier stable isotope to the lighter stable isotope in a sample or standard.

The δ values for stable-isotope ratios discussed in this report are referenced to the following standard materials:

Element	R	Standard identity and reference
boron	boron-11/boron-10 ($\delta^{11}\text{B}$)	National Bureau of Standards—Standard Reference Material 951 (Bassett, 1990)
carbon	carbon-13/carbon-12 ($\delta^{13}\text{C}$)	Pee Dee Belemnite (Fritz and Fontes, 1980)
hydrogen	hydrogen-2 (deuterium)/hydrogen-1 (δD)	Vienna Standard Mean Ocean Water (Fritz and Fontes, 1980)
oxygen	oxygen-18/oxygen-16 ($\delta^{18}\text{O}$)	Vienna Standard Mean Ocean Water (Fritz and Fontes, 1980)
sulfur	sulfur-34/sulfur-32 ($\delta^{34}\text{S}$)	Canyon Diablo Troilite (Fritz and Fontes, 1980)

The other isotope ratios used in this report are referenced as follows:

Element	R	Standard identity and reference
carbon	carbon-14/carbon $\times 100$ (^{14}C)	Not applicable
strontium	strontium-87/strontium-86 ($^{87}\text{Sr}/^{86}\text{Sr}$)	National Institute of Standards and Technology—Standard Reference Material 987 (Fritz and Fontes, 1980)
chlorine	chlorine-36/chlorine ($^{36}\text{Cl}/\text{Cl}$)	Swiss Federal Institute of Technology, Zurich—sample ETHB-1 (George Vourvopoulos, Western Kentucky University, written commun., 1992)

Abbreviations:

°C, degree Celsius
km, kilometer
L, liter
m, meter
mg, milligram
mg/L, milligram per liter
mL, milliliter
MPa, megaPascal
m²/d, meter squared per day
m³, cubic meter
m³/yr, cubic meter per year
μm, micrometer
μS/cm, microsiemens per centimeter at 25 degrees Celsius

Hydrogeologic Framework and Geochemistry of the Edwards Aquifer Saline-Water Zone, South-Central Texas

By George E. Groschen *and* Paul M. Buszka

Abstract

The Edwards aquifer supplies drinking water for more than 1 million people in south-central Texas. The saline-water zone of the Edwards aquifer extends from the downdip limit of freshwater to the southern and eastern edge of the Stuart City Formation. Water samples from 16 wells in the Edwards aquifer saline-water zone were collected during July–September 1990 and analyzed for major and minor dissolved constituents, selected stable isotopes, and radioisotopes. These data, supplemental data from an extensive water-quality data base, and data from other previous studies were interpreted to clarify the understanding of the saline-water-zone geochemistry.

Most of the isotope and geochemical data indicate at least two distinct hydrological and geochemical regimes in the saline-water zone of the Edwards aquifer. On the basis of hydrogen and oxygen isotopes and radiocarbon data, the shallower updip regime is predominantly meteoric water that has been recharged probably from the freshwater zone within recent geologic time (less than tens of thousands of years). Also, on the basis of hydrogen and oxygen isotope data, water in the hydrologically stagnant regime (downdip) has been thermally altered in reactions with the carbonate rocks of the zone. The deeper water probably is much older than water in the shallow zone and is nearly stagnant relative to that in the shallow zone.

The geochemical grouping observed in the well-water data from well samples in the saline-water zone indicates that the zone is hydrologically compartmentalized, in part because of faults that function as barriers to downdip flow of recharge water. These fault barriers also probably impede updip flow. Flow compartmentalization and the resulting disparity in geochemistry between the two regimes indicate that updip movement

of substantial amounts of saline water toward the freshwater zone is unlikely.

Estimated in-place temperature of the samples collected indicates an increase with depth and (or) distance from the downdip limit of freshwater. The pH of the samples decreases with increasing distance from the downdip limit of freshwater, but the decrease is caused partly by the increase in temperature. Dissolved major ions and dissolved solids concentrations all indicate a progressive but monotonic increase in salinity from updip to downdip. The alkalinity of the water samples is predominantly bicarbonate because the low-molecular weight aliphatic-acid anion concentrations are small relative to the bicarbonate concentrations. The dissolved organic carbon concentrations also are lower than expected for an aquifer with economic amounts of oil and gas hydrocarbons.

INTRODUCTION

The Edwards aquifer in south-central Texas (fig. 1) supplies more than 1 million people in the San Antonio metropolitan area with water for public supply, industry, and irrigation. The aquifer has freshwater and saline-water zones. The freshwater/saline-water interface is known locally as the bad-water line and hereafter is referred to as the "downdip limit of freshwater." The downdip limit of freshwater in the aquifer is the approximate surface defined by the 1,000-mg/L dissolved solids concentration. Perez (1986) reported that, under certain conditions, the movement of saline water into the freshwater zone is possible.

Because the Edwards aquifer is the public water supply for more than 1 million people, it is critical to know (1) whether saline water will move into the freshwater zone, and (2) if it does, where, how rapidly, and in what quantity. Should saline-water intrusion occur, the extensively leached freshwater part of the aquifer might

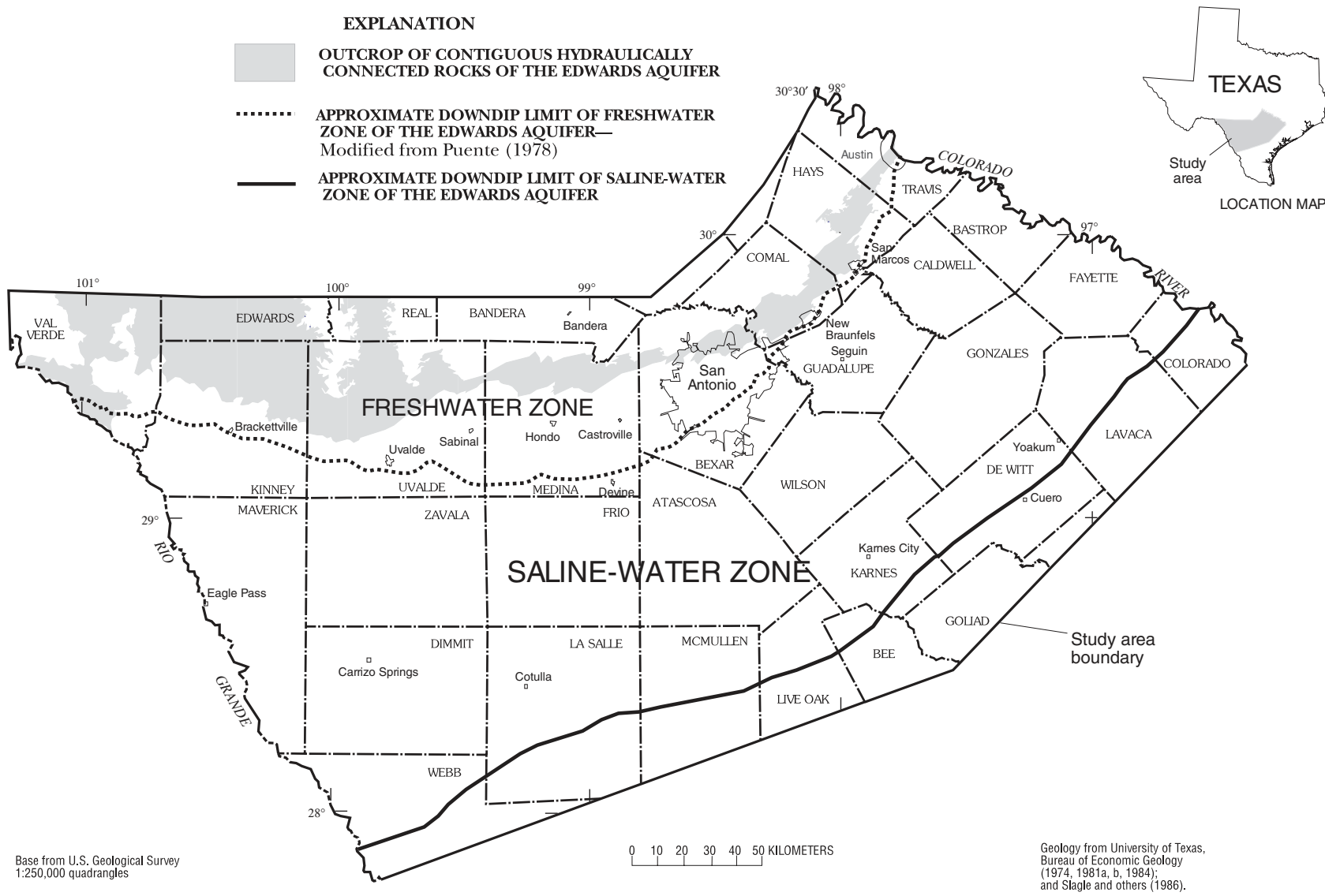


Figure 1. Location of the study area.

allow mixing of the saline water and freshwater. The mixing of freshwater and saline water could contaminate sections of the most productive area of the aquifer near San Antonio and northeastward toward the major springs at New Braunfels and San Marcos (fig. 1).

The freshwater part of the Edwards aquifer is approximately 370 km long from west to northeast and about 16 to 65 km wide. The freshwater part of the aquifer is bounded to the north by the edge of the recharge zone (shown as the outcrop area in fig. 1) and to the south and southeast by the downdip limit of freshwater. At the downdip limit of freshwater near San Antonio, the top of the Edwards aquifer is about 300 m below land surface and the aquifer is about 150 m thick.

As described in this report, the saline-water zone of the Edwards aquifer extends from the downdip limit of freshwater to the southern and eastern edge of the Stuart City Formation (shown as the downdip limit of the saline-water zone in fig. 1). The freshwater zone includes the recharge zone and the confined part of the aquifer that contains water with dissolved solids concentration less than 1,000 mg/L. Freshwater is defined as having a dissolved solids concentration of less than 1,000 mg/L, and saline water is defined as having a dissolved solids concentration of 1,000 mg/L or greater. "Slightly saline" and "brine" refer to the opposite extremes of the range of saline-water concentrations. Brine is defined as having a dissolved solids concentration greater than 35,000 mg/L.

In 1985, the U.S. Geological Survey (USGS), in cooperation with the Edwards Aquifer Authority and the San Antonio Water System, began a study to improve the definition of the downdip limit of freshwater and to assess the potential for saline-water movement into the freshwater zone. Data collected during drilling of monitor wells across the downdip limit of freshwater are published in Pavlicek and others (1987) and Poteet and others (1992) and are interpreted in William F. Guyton Associates, Inc. (1986) and Groschen (1994).

Purpose and Scope

This report describes the hydrogeologic framework and geochemistry of the Edwards aquifer from the downdip limit of freshwater to the downdip limit of the saline-water zone with emphasis on general geology, geochemical equilibria, spatial distribution of dissolved constituents, and geochemical processes that might be affecting water composition. The report includes a com-

pilation and interpretation of historical geochemical data. Data for this study were collected during September 1987–September 1991. Data from three well transects across the downdip limit of freshwater also were used. The well transects are in San Antonio, in New Braunfels near Comal Springs, and in San Marcos near San Marcos Springs.

Methods of Data Collection and Analysis

Historical geologic, water-chemistry, and water-salinity data were compiled from published sources. Water-quality and water-level data were collected from (1) transect monitor wells at the downdip limit of freshwater, and (2) wells in the saline-water zone; the data were used to define further possible chemical reactions and to classify and (or) date the water in the saline-water zone. The well transects cross the downdip limit of freshwater at three locations. The San Antonio transect of monitor wells consists of seven wells in three nests of vertically discrete piezometers (Pavlicek and others, 1987). The New Braunfels transect consists of five wells in two nests and a single well about 1.6 km south-southeast of Comal Springs (Poteet and others, 1992). The northernmost transect consists of four wells in two nests and a single well near San Marcos Springs in San Marcos (Poteet and others, 1992). The wells in the saline-water zone consist of 6 wells near the downdip limit of freshwater and 10 oil or gas wells.

Sampling Methods

The seven wells in the San Antonio transect were sampled quarterly during April 1987–January 1988 and monthly during January 1988–October 1991 (Nalley, 1989; Nalley and Thomas, 1990; Brown and others, 1991 and 1992). The five wells in the New Braunfels transect were sampled quarterly during September 1989–October 1991, and the four wells in the San Marcos transect were sampled quarterly during 1991 (Brown and others, 1991 and 1992). The 16 wells in the saline-water zone were sampled during July–September 1990.

Water samples were collected from the transect wells of the Edwards aquifer using procedures described in Wood (1976) and Claassen (1982). If the hydraulic head at the site was above land surface, the well bore was purged of stagnant water by pumping or by opening a valve at the wellhead. Specific conductance, pH, and temperature were monitored in the effluent water for at least 15 minutes until stable values were

measured. Water samples then were collected from the well and filtered. Water samples from the transect wells were filtered through membranes with a pore size of 0.45 μm .

Water samples were collected from the transect wells for field titration of alkalinity and for laboratory analysis of major ion concentrations. Alkalinity determinations were done on unfiltered water samples by use of incremental titrations, as described in Wood (1976). Each of the transect wells was sampled annually for determination of trace elements and several stable isotopes. In addition, two wells in the San Antonio transect were sampled three times for carbon-14 (^{14}C) analyses.

Water samples were collected from oil wells in the saline-water zone of the Edwards aquifer using procedures modified from Lico and others (1982). The wells were selected by location, availability of information, and accessibility. Saline-water-zone wells selected for sampling commonly produced more than 1.6 m^3 of brine per hour. Ratios of brine to oil produced from these wells were greater than about 10:1. The brine-oil mixture was collected from these wells from a sample tap at the wellhead before being routed to separation or processing equipment. The brine-oil mixture was collected in four 50-L polyethylene carboys. The carboys had been prewashed with phosphate-free detergent and thoroughly rinsed with tap water and deionized water before each use. Each carboy was filled to the brim, sealed with a threaded cap, and allowed to stand for 2 to 3 hours until the brine and oil had separated substantially. The brine was drained from a spout at the base of each carboy to minimize oil entry to the sample.

Water samples from the 16 saline-water-zone wells were filtered using polycarbonate filter media with a pore size of 0.1 μm . Analyses for dissolved ferrous and ferric iron and dissolved sulfide were done at the site by colorimetric methods (Hach Co., 1989; S.K. Anderholm and P.M. Buszka, U.S. Geological Survey, written commun., 1990). All field analyses were done within one-half hour after sample processing began. Filtered water samples were collected for determination of major and minor dissolved constituents, stable isotopes, and radioisotopes.

Sample Preparation and Laboratory Analyses

Standard analytical procedures were used for laboratory determinations of the concentrations of dissolved constituents including major cations (calcium, magnesium, sodium, and potassium), sulfide, major

anions (sulfate and chloride), trace elements (boron, bromide, iodide, iron, lithium, strontium, and trace metals), and organic carbon (Wershaw and others, 1987; Fishman and Friedman, 1989). The containers used for sample collection and the treatments used for sample preservation are summarized in Pritt and Jones (1990). L.S. Land (Department of Geology, University of Texas at Austin) made replicate determinations of major inorganic ions from several of the samples.

On the basis of results published by Fisher (1987), it was assumed that aliphatic-acid anions could represent a substantial proportion of the alkalinity (as determined by onsite titrations) in saline-water zones. Water samples collected from the transect wells were placed in 1-L, precleaned, brown glass bottles for determination of low-molecular-weight aliphatic acids. The laboratory procedures (gas chromatography with flame-ionization detection) are described in American Public Health Association and others (1989). The aliphatic acids analyzed for were acetic, propionic, isobutyric, n-butyric, and n-valeric. Analyses for the aliphatic acids were done at the Lower Colorado River Authority Laboratory in Austin, Tex.

Stable-isotope determinations requiring limited special treatment of samples included those for boron ($\delta^{11}\text{B}$), oxygen ($\delta^{18}\text{O}$), hydrogen (δD), and absolute ratios of strontium ($^{87}\text{Sr}/^{86}\text{Sr}$). Water samples for boron and strontium stable-isotope determinations were placed in 1-L polyethylene bottles. Water samples for oxygen and hydrogen stable-isotope determinations were placed in 125-mL glass bottles with polyseal caps and were preserved by refrigeration.

Water samples for analyses of stable-isotope ratios of dissolved inorganic carbon and dissolved sulfate and sulfide required special treatment. Samples for carbon ($\delta^{13}\text{C}$) analysis were treated with ammoniacal strontium chloride solution in 1-L glass bottles and preserved with a mercuric chloride tablet before refrigeration and shipment. Samples for sulfur ($\delta^{34}\text{S}$) analysis of dissolved sulfate were treated with barium chloride to precipitate barium sulfate and were filtered to separate out the solid; afterwards, the solid and filter were transferred to a 40-mL glass vial (R. W. Carmody, Eurybiades Busenberg, L.N. Plummer, and T.B. Coplen, U.S. Geological Survey, written commun., 1993). Samples for $\delta^{34}\text{S}$ analysis of dissolved sulfide were purged from 50- to 150-L water samples by use of nitrogen gas through a 10-percent silver nitrate solution and were filtered to separate the silver sulfide precipitate.

The barium sulfate and silver sulfide precipitates were analyzed for $\delta^{34}\text{S}$ by mass spectrometry by W.C. Shanks III (U.S. Geological Survey, Isotope Geochemistry Laboratory, Reston, Va.). Water samples were analyzed for $\delta^{13}\text{C}$ in inorganic carbon by mass spectrometric methods by A.F. White (U.S. Geological Survey, Branch of Regional Research Laboratories, Menlo Park, Calif.). Water samples for $\delta^{11}\text{B}$ and $^{87}\text{Sr}/^{86}\text{Sr}$ analysis were collected from untreated samples and sent to L.S. Land (Department of Geology, University of Texas at Austin).

Tritium analyses were done on untreated samples that were collected in glass bottles with polyseal caps (Pritt and Jones, 1990). The samples were electrolytically enriched prior to mass spectrometric analysis (Thatcher and others, 1977).

Samples for ^{14}C analysis were collected in the field as a strontium carbonate precipitate using a method modified from Thatcher and others (1977). The ^{14}C determinations were done on solid strontium carbonate precipitated in the field. A 100-L closed funnel was filled with sample water, and air was excluded. Excess strontium chloride solution and ferrous ammonium sulfate solutions were added sequentially. Sodium hydroxide solution was added to adjust the pH to precipitate all the dissolved inorganic carbon in the water. After several hours of settling, the precipitate was removed from the bottom of the funnel and sealed in 1-L polyethylene bottles for shipment. The details of the analytical procedure are described in Thatcher and others (1977).

Water samples from the saline-water zone for determination of absolute ratios of chlorine ($^{36}\text{Cl}/\text{Cl}$) of dissolved chloride were collected in 1-L bottles, left untreated, and then sent to George Vourvopoulos (Department of Physics and Astronomy, Western Kentucky University) for preparation and analysis. Each sample was first repeatedly treated to minimize all dissolved sulfur species to a total concentration of less than 1 mg/L. Final preparation of the water samples consisted of chemically precipitating the dissolved chloride as silver chloride in concentrations ranging from 100 to 300 mg per sample. George Vourvopoulos (Department of Physics and Astronomy, Western Kentucky University) did the analysis on the dedicated accelerator/mass spectrometry facility at the Swiss Federal Institute of Technology, Zurich, Switzerland.

The $^{36}\text{Cl}/\text{Cl}$ of each of the samples was measured in two independent runs. Two of the samples (S-13 and S-15) were prepared and run at different times. Samples

S-13 and S-15 were prepared and run in November 1990, and samples S-13R and S-15R were prepared from a different water sample and were run in February 1991. The repeatability of the measurements was extremely good despite the low ^{36}Cl concentration.

Two blanks with known $^{36}\text{Cl}/\text{Cl}$ ratios were prepared and run. One blank was prepared from salt available at the Swiss Federal Institute of Technology, Zurich (sample ETHB-1), and another blank was prepared from halite from the Weeks Island salt dome in Louisiana (sample LABK-1). Many samples of the halite have been analyzed at laboratories in Australia and in Rochester, N.Y. Depending on the sample and the time it remained in a desiccator, $^{36}\text{Cl}/\text{Cl}$ ratios have ranged from 2×10^{-15} to 10×10^{-15} (George Vourvopoulos, Department of Physics and Astronomy, Western Kentucky University, written commun., 1992). Because the $^{36}\text{Cl}/\text{Cl}$ ratios in many samples have been smaller than those in the Weeks Island halite, and because of the demonstrated high replicability of the analytical technique, the ETHB-1 sample becomes the background correction sample. The errors in the measurements include statistical error and uncertainty in the standard correction. The values for ^{36}Cl atoms per liter were derived from chloride concentrations determined by independent analysis.

Water samples collected for determination of dissolved gases were analyzed by two methods. The primary method involved a laboratory-supplied glass tube with an evacuated side tube and dual-valve stopcocks (Hobba and others, 1977). Several volumes of ground water were flushed through the main tube with the stopcocks to the side glass tube closed. After all air bubbles were purged and several liters of overflow had passed through the large tube, the two stopcocks were turned 90 degrees to stop flow and seal the tube. The stopcocks were rotated to open the water-filled large tube to the evacuated side-arm tube to allow evolution of gases into the sidearm. The stopcocks were closed and bound to prevent loosening during transport. Ray Van Hoven (U.S. Geological Survey, Reston, Va.) analyzed the gas samples for dissolved nitrogen (N_2), oxygen (O_2), argon (Ar), carbon dioxide (CO_2), ethane (C_2H_6), methane (CH_4), and hydrogen sulfide (H_2S) using gas chromatography with a thermal conductivity detector. Other gas samples were collected in stainless steel gas tubes, left untreated, and analyzed for hydrocarbon gases and the $\delta^{13}\text{C}$ of the gas phase by L.S. Land (Department of Geology, University of Texas at Austin).

Well-Numbering System

The well-numbering system in Texas was developed by the Texas Water Development Board for use throughout the State (fig. 2). Under this system, each 1-degree quadrangle was given a two-digit number from 01 through 89. These are the first two digits of the well number. Each 1-degree quadrangle is divided into 7–1/2-minute quadrangles (similar to the 1:24,000 topographic quadrangle sheets), and each 7–1/2-minute quadrangle is assigned another two-digit number from 01 through 64. These are the third and fourth digits of the well identification number. Each 7–1/2-minute quadrangle is divided into 2–1/2-minute quadrangles numbered 1 through 9 for the fifth digit of the well number. As each well within a 2–1/2-minute quadrangle is inventoried (beginning about 1965), a number from 01 to 99 is appended to the one-digit 2–1/2-minute quadrangle for the last three digits of the well number.

In addition, each county in Texas is assigned a unique two-letter code. The county code is placed at the beginning of the well number. In the study area, the two-letter county codes include: AL, Atascosa County; AY, Bexar County; BU, Caldwell County; DX, Comal County; KR, Gonzales County; KX, Guadalupe County; LR, Hays County; PZ, Karnes County; YP, Uvalde County; and ZX, Zavala County.

Acknowledgments

The authors extend thanks to the well owners and the companies who allowed USGS personnel access to their wells and properties.

HYDROGEOLOGIC FRAMEWORK

Geology and Stratigraphy of Aquifer Units

The Edwards aquifer comprises all or most of seven geologic formations as defined by Lozo and Smith (1964) and Rose (1972): the Kainer, Person, and Georgetown Formations in the eastern one-half of the study area; the Devils River Formation in the central part of the study area; and the West Nueces, McKnight, and Salmon Peak Formations in the western part (fig. 3). The saline-water zone of the aquifer also contains the Stuart City Formation.

Regional stratigraphic studies of the formations of the Edwards aquifer by Rose (1972) and studies of equivalent rocks in south Texas by Winter (1961), Tucker (1962), Lozo and Smith (1964), and Fisher and

Rodda (1969) have resulted in subdivisions within the major depositional provinces and correlations among the provinces. Rose (1972) divided the former Edwards Limestone into the Kainer and Person Formations. The stratigraphically equivalent units that compose the Edwards aquifer are the Kainer and Person Formations and the overlying Georgetown Formation in the San Marcos platform depositional province (fig. 4); the Devils River Formation of the Devils River trend depositional province; the West Nueces, McKnight, and Salmon Peak Formations of Lozo and Smith (1964) in the Maverick Basin depositional province; and the laterally juxtaposed part of the Stuart City Formation in the Stuart City reef trend depositional province (Bebout and Loucks, 1974).

All the formations that compose the Edwards aquifer are either limestone or dolostone. In the freshwater zone, most of the dolostone has been converted to calcic limestone, a process called diagenesis. Most of the stratigraphic characteristics of the aquifer subdivisions described by Maclay and Small (1984) for the freshwater zone also are descriptive of the saline-water part of the aquifer, but aquifer materials in the saline-water zone are not modified by diagenesis to the extent observed in the freshwater zone (Mench-Ellis, 1985; Deike, 1990). Geologic data for the thickness of each formation were obtained from geophysical logs and from Winter (1961), Tucker (1962), Rose (1972), and Bebout and Loucks (1974).

Kainer, Person, and Georgetown Formations

The Kainer Formation, as defined by Rose (1972), is about 100 m thick and consists of four informal members. The basal nodular member (fig. 3) is a marine deposit consisting of massive, nodular wackestone. The dolomitic member consists of burrowed and dolomitized wackestone with substantial porosity. The upper part of the dolomitic member contains leached evaporitic deposits of the Kirschberg evaporite. The uppermost member of the Kainer Formation (grainstone member) is a shallow marine deposit of well-cemented, miliolid grainstone with small amounts of mudstone (Rose, 1972).

The Person Formation is about 55 m thick where it is not eroded, and it consists of five informal members (Rose, 1972). The basal member (regional dense member) is a laterally extensive marine deposit of dense, shaly mudstone. The leached and collapsed members are intertidal to supratidal deposits, containing collapse

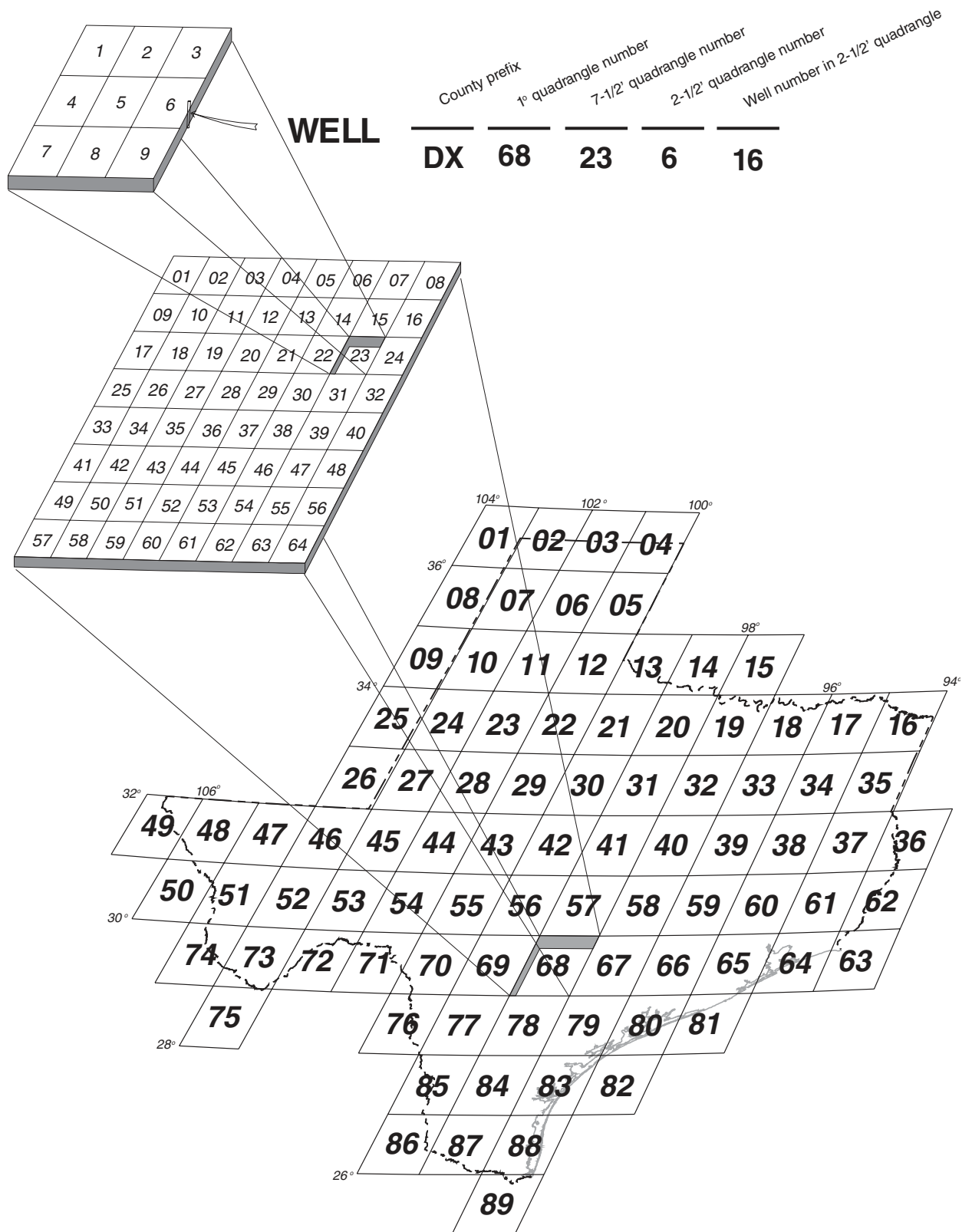
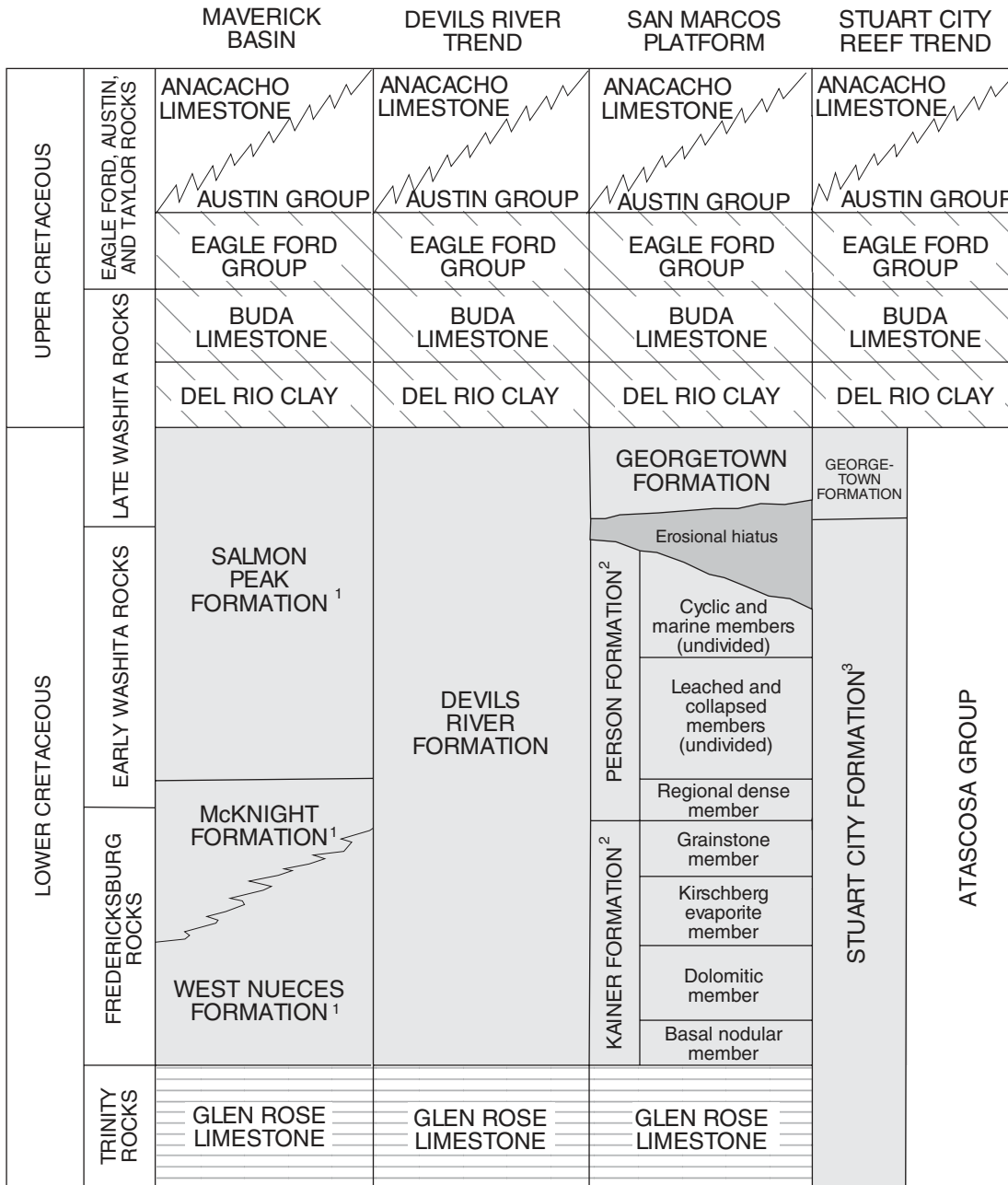


Figure 2. Diagram showing well-numbering system.

ROCK FACIES



¹ Of Lozo and Smith (1964).
² Modified from Rose (1972).
³ Bebout and Loucks (1974).

EXPLANATION

- Upper confining unit
- Edwards aquifer
- Lower confining unit

Figure 3. Correlation of Cretaceous stratigraphic units in south Texas and Edwards aquifer hydrostratigraphic units in the San Marcos platform area, south-central Texas.

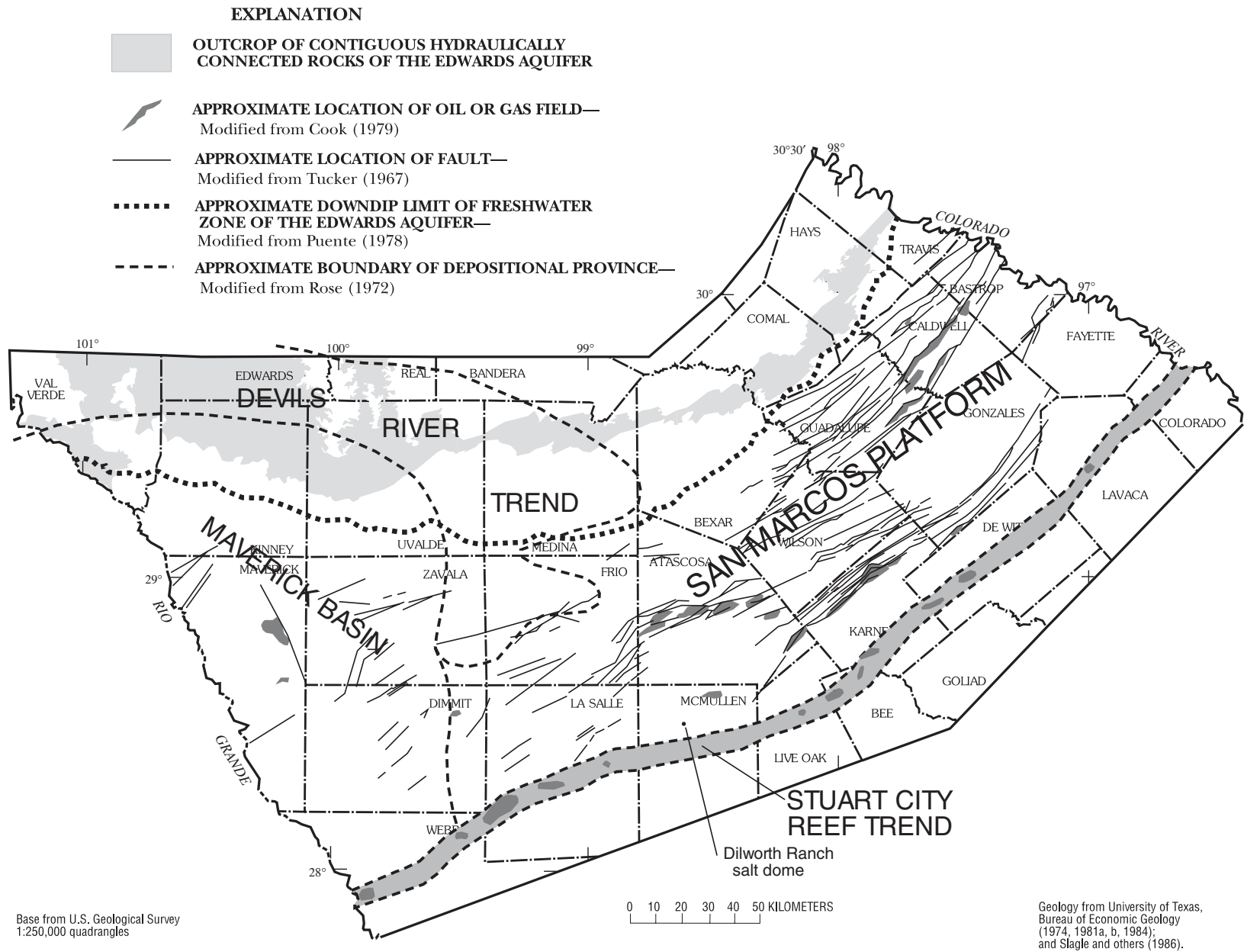


Figure 4. Location of selected faults, oil and gas fields, and depositional provinces near the Edwards aquifer saline-water zone, south-central Texas.

breccias and dolomitized and burrowed wackestone. The uppermost member that can be identified in cores is the marine member of rudist-bearing wackestone and shell-fragment grainstone. The cyclic member is located in parts of the saline-water zone, but it is mostly absent from the crest of the San Marcos platform because of erosion prior to deposition of the Georgetown Formation (fig. 3).

The Georgetown Formation ranges in thickness from about 80 m in deeply buried troughs in the saline-water zone to less than 25 m on the upthrown edges of fault blocks (Rose, 1972). At land surface, the Georgetown Formation is mostly to completely eroded and is present only in small, isolated locations (W.G. Stein and G.B. Ozuna, U.S. Geological Survey, written commun., 1991).

Devils River Formation

Lozo and Smith (1964) defined the Devils River Formation as rocks with the same stratigraphic interval as the Kainer, Person, and Georgetown Formations but without any consistent markers to subdivide the formation. The basal section, above the contact with the Glen Rose Limestone, is about 21 m of nodular, dense, shaly limestone that grades upward into 70 m of tidal and marine wackestone and mudstone. Above these rocks is about 12 m of mudstone and collapse breccias. The upper 60 m is shallow marine deposits consisting of biohermal rudist mounds, talus grainstone, and interreefal wackestone (Maclay and Small, 1984).

West Nueces, McKnight, and Salmon Peak Formations

The deposits of the Maverick Basin where the West Nueces, McKnight, and Salmon Peak Formations were formed primarily are dense, homogeneous, fine-grained limestone and dolostone with minimal primary porosity (Maclay and Small, 1984). The West Nueces Formation in Uvalde County consists of 18 m of nodular, shaly limestone in the lower part and 24 m of pelleted, shell-fragment wackestone and some grainstone. The upper part also contains beds of dolomitized, burrowed wackestone.

The McKnight Formation consists of upper and lower units of thinly bedded limestone separated by a black, fissile, clayey, lime mudstone about 8 m thick. The lower unit is about 21 m of dense, fecal-pellet mudstone and shell-fragment grainstone interbedded with collapse breccias. The upper unit consists of

about 17 m of thinly bedded mudstone and associated evaporite.

The Salmon Peak Formation is about 90 m of dense, massive, lime mudstone containing chert in the lower part and about 23 m of layered to crossbedded, rounded, shell-fragment grainstone.

Stuart City Formation

The Stuart City Formation was deposited contemporaneously with the Glen Rose Limestone, West Nueces, McKnight, and Salmon Peak Formations, the Devils River Formation, and the Kainer and Person Formations (Bebout and Loucks, 1974). The Stuart City barrier reef created the back-reef shallow-water area for the deposition of those formations. The Georgetown Formation overlaps the top of the Stuart City Formation (Rose, 1972; Bebout and Loucks, 1974). The Stuart City Formation ranges from about 610 to 760 m in thickness and generally is buried at a depth of 3,400 to 6,100 m. The formation is a complex mixture of shallow-water reefal deposits and slightly deeper water reef grainstone and debris. Although primary porosity in some zones ranges from 30 to 40 percent, these zones are small and isolated. Much of the primary porosity in the formation is less than 30 percent, owing to occlusion by cements (Bebout and Loucks, 1974).

Stratigraphy of Underlying and Overlying Units

Glen Rose Limestone

The geologic unit stratigraphically below the Edwards aquifer is the Glen Rose Limestone. The total thickness of this formation is at least 365 m. The Glen Rose is composed of a sequence of calcareous shale, limestone, and dolostone in the upper part and massive-bedded limestone and dolostone in the lower part.

Del Rio Clay, Buda Limestone, and Eagle Ford Group

The Del Rio Clay is dark-gray, calcareous shale that is predominantly argillaceous. The Del Rio Clay generally is about 13 to 18 m thick near the updip limit of the saline-water zone, but it is only about 3 to 6 m thick near the Stuart City reef trend. It is absent in small parts of the saline-water zone, especially over the Stuart City Formation. The Buda Limestone is similar to the Georgetown Formation and generally is about 25 to 37 m thick, although it is less than 18 m thick in some

areas. The Eagle Ford Group is about 9 m thick near the updip limit of the saline-water zone and about 75 m thick near the Stuart City reef trend. The Eagle Ford Group consists of shale, siltstone, and limestone; flaggy limestone beds are interbedded with carbonaceous shale. Each of these three units thickens over the Maverick Basin depositional province.

Geologic Structure and Faults

Numerous faults in the study area divide the saline-water zone of the Edwards aquifer into many smaller blocks. Only those mapped faults in the saline-water zone of the aquifer are shown in figure 4. The vertical displacement along many of these near-vertical to vertical faults ranges from slightly less than to much greater than the thickness of the aquifer. The combination of up-to-coast and down-to-coast faults in the saline-water zone have a net total displacement of about zero (Tucker, 1967). Similar faults in the freshwater zone act as barriers to ground-water flow (Maclay and Land, 1988, p. A17, A19).

Hydrologic Framework

The hydrology of the saline-water zone of the Edwards aquifer depends to a large degree on the hydrologic conditions. The diagenesis that created the high-calcium limestone also created the large effective porosity and large transmissivity of the freshwater zone, but diagenesis has not substantially affected the saline-water zone (Maclay and Small, 1984; Mench-Ellis, 1985; Deike, 1990). The permeability on the saline-water side of the downdip limit of freshwater is at least 2 to 3 orders of magnitude less than the permeability on the freshwater side (Maclay and Land, 1988). Transmissivity in the freshwater zone near the downdip limit of freshwater is as great as 190,000 m²/d (Maclay and Small, 1984, p. 50). Transmissivity on the saline-water side of the downdip limit of freshwater is not known, but it has been estimated to be about 1,000 m²/d or less (William F. Guyton Associates, Inc., 1986, p. 25). Effective porosity in the saline-water zone is poorly defined but likely is less than 10 percent. The velocity of flow is much slower in the saline-water zone than in the freshwater zone because of the lower permeability of the saline-water zone; therefore, the residence time of saline water is much longer than in the freshwater zone.

A geopressured zone, where fluid pressures are greater than that of hydrostatic and lithostatic overburden, is present in Gulf Coast clastic sediments east of

the Edwards aquifer saline-water zone and 500 m or more higher in the stratigraphic section. The updip limit of the geopressured zone lies in the subsurface Cenozoic aquifers approximately above the Stuart City Formation (Williamson and others, 1990). The relative locations of the saline-water zone of the Edwards aquifer and the geopressured zone are shown in a generalized hydrogeologic section of southwestern Texas approximately where it is closest to the Edwards aquifer (fig. 5). The Upper Cretaceous and Tertiary geologic formations between the Edwards aquifer and the bottom of the geopressured zone contain hundreds of meters of limestone and shale. Available data are insufficient to indicate whether geopressured zones are present in Cretaceous sediments in the Gulf of Mexico Basin.

Recharge to and discharge from the saline-water zone primarily is flow across the downdip limit of freshwater (Maclay and Land, 1988). The amount of recharge from the freshwater zone is unknown but likely is less than about 10 percent of the annual recharge to the freshwater zone; total recharge to the freshwater zone averages about 790 million m³/yr (Nalley, 1989, p. 14–15). The net flux across the downdip limit of freshwater (flow of freshwater out and saline water in) might be close to zero and thus inconsequential in terms of the water budget for the freshwater zone.

In addition, some water probably flows into the Edwards aquifer saline-water zone from other formations below the upper Glen Rose Limestone (Trinity aquifer) or from above the Eagle Ford Group. The rate of flow from the Edwards aquifer into underlying or overlying aquifers is unknown. A few saline-water wells near the downdip limit of freshwater are allowed to flow at rates less than a few liters per second. The amount and location of natural saline-water discharge is unknown.

Land and Prezbindowski (1981, 1985) and Clement and Sharp (1988) have inferred that recharge to the Edwards aquifer saline-water zone from deeper formations has occurred or could occur along faults. Faults are assumed to be at least episodically permeable to brines from other aquifers where discharge of fluid results from sediment compaction or geopressured conditions. The basis for postulating upward flow of brines along faults is the unusual chemistry of the Edwards aquifer saline-water-zone brines. At least one salt dome (Dilworth Ranch salt dome) pierces the Edwards aquifer saline-water zone (fig. 4). Hanor (1987a) concluded that salt dissolution in highly faulted zones around salt

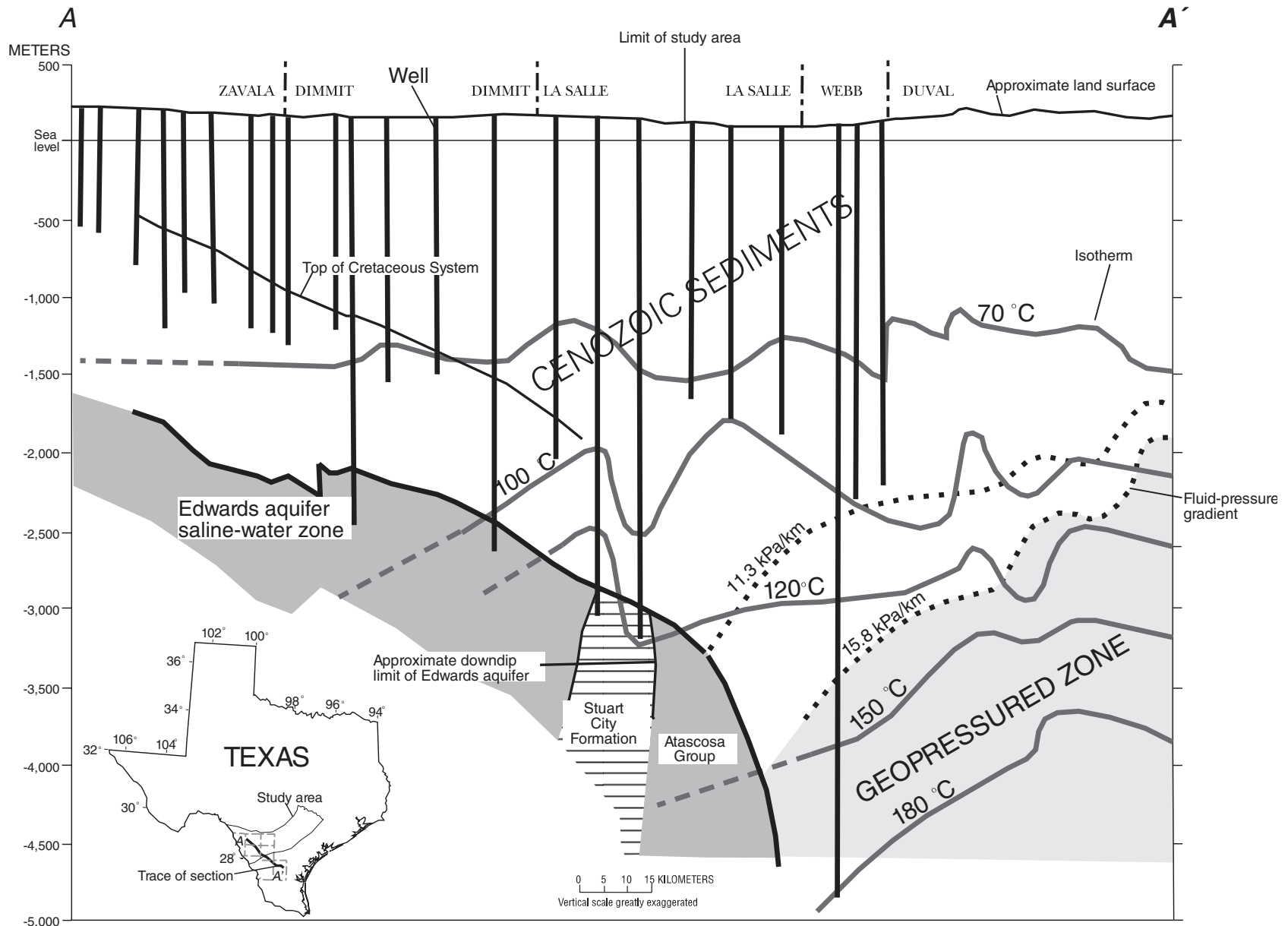


Figure 5. Generalized hydrogeologic section showing the relation between the Edwards aquifer and the geopressured zone in the subsurface of the Texas Gulf Coast.

domes can create vertical flow systems that transgress stratigraphic boundaries. The volume and timing of brine intrusion by either of these mechanisms in the study area is unknown.

Other sources of recharge to and discharge from the saline-water zone include the production and injection of brines from oil and gas wells. Dedicated disposal wells are used to inject local waste brine from oil and gas production from the Edwards aquifer. Generally, waste brine from the Edwards aquifer saline-water zone is reinjected into the deepest parts of the aquifer. Amounts of produced waste brine can be as great as 100 parts of brine per 1 part of crude oil (Cook, 1979). Injection of waste brine from sources other than oil and gas wells in the Edwards aquifer saline-water zone is assumed to be inconsequential.

GEOCHEMISTRY OF THE SALINE-WATER ZONE

Concentration data for dissolved solids and major ions of the saline-water zone are from a computer data base of saline-water chemical data (Taylor, 1975; Pettijohn, 1986). In this report, these data are collectively referred to as the "TP file." The data in the TP file came from various sources, including the USGS. The uncertainty for dissolved solids and dissolved chloride determinations is small. The specific uncertainty of the other ion determinations is unknown, but was assumed to be sufficiently small to allow for interpretation. The locations of the wells selected from the TP file that were sampled and analyzed for most major ions and dissolved solids are shown in figure 6. The locations of the 16 saline-water-zone wells sampled in 1990 (including wells from three transects) and the three transects are shown in figure 7. Well construction, physical characteristics, pH, and major-ion concentration data for the 16 wells sampled during July–September 1990 are listed in tables 1–2. Distributions of dissolved solids and major ions are discussed in order of importance in a subsequent section of this report.

The geochemical grouping observed in the data from well samples in the saline-water zone indicates that the zone is hydrologically compartmentalized. In the following discussion of the geochemical and isotope data, samples from the 16 saline-water-zone wells are separated into three groups that generally correspond to the distance from the downdip limit of freshwater. The first group—the transition group—comprises samples from wells near the downdip limit of freshwater (wells

1, 2, 5, 8, 12, and 17). The second group—the shallow oil and gas wells—comprises samples from wells 3, 7, 14, and 15. The first and second groups combined form the hydrologically active group. The third group—the hydrologically stagnant group—comprises samples from wells 4, 6, 10, 11, 13, and 16.

Equilibrium Species Distribution

Application of Equilibrium-Computation Program

SOLMINEQ.88 (SOLution MINeral EQUilibrium) (Kharaka and others, 1988) is a general, comprehensive computer program for computing dissolved species distribution, mineral saturation states, and geochemical reaction models for water-rock interactions. SOLMINEQ.88 is particularly suited for applications involving water in sedimentary basins and in thermally stimulated oil reservoirs where petroleum and aqueous organic species play an important role. The thermodynamic data base included data for 260 inorganic aqueous species, 80 organic aqueous species, and 220 minerals that allow the program to compute pH and mineral saturation states at given subsurface temperatures and pressures.

SOLMINEQ.88 was used to determine the distribution of dissolved inorganic species, to adjust subsurface temperature corrections on the basis of the relative proportions of major ions and silica, and to correct pH for adjusted subsurface temperatures, as well as to estimate mineral saturation states, or saturation indices (SIs). SOLMINEQ.88 computes these various values at high temperatures and pressures using approximate Pitzer equations (Kharaka and others, 1988) for estimating ion activities in brine. The activity ratio of dissolved magnesium and calcium also was computed because the stability of the minerals dolomite and calcite are of great interest in the Edwards aquifer saline-water zone.

The SI is defined as the \log_{10} (dimensionless) of the ratio of the activity product of the dissolved species to the equilibrium constant for a specific mineral at the temperature and pressure of the sample. An SI of zero indicates precise equilibrium, greater than about 0.10 indicates supersaturation with respect to the mineral, and less than about -0.10 indicates undersaturation. The mineral saturation states, as SIs, for the 16 water samples collected are listed in table 3.

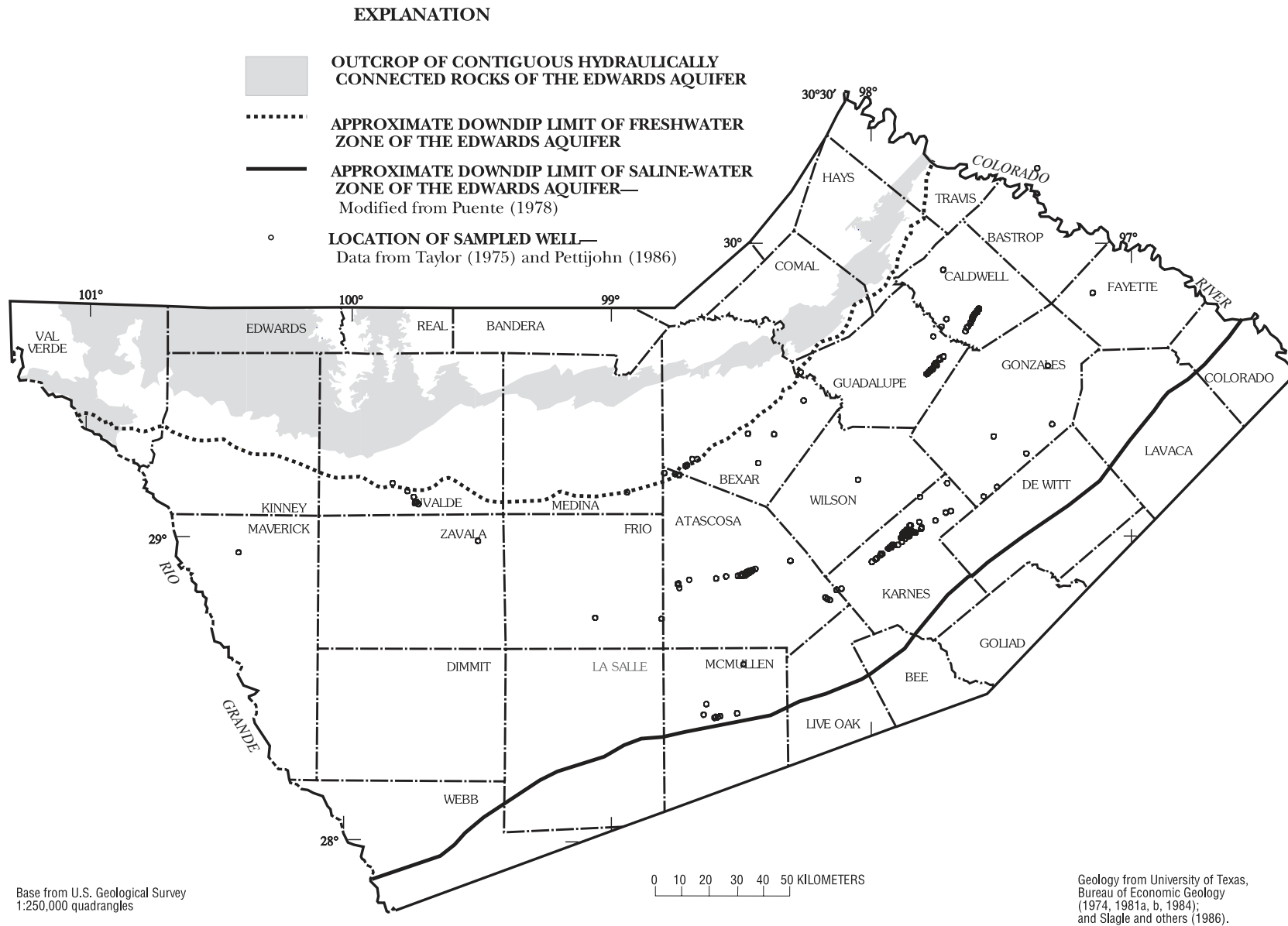


Figure 6. Location of wells in the Edwards aquifer saline-water zone, south-central Texas, for which water-sample analyses are available.

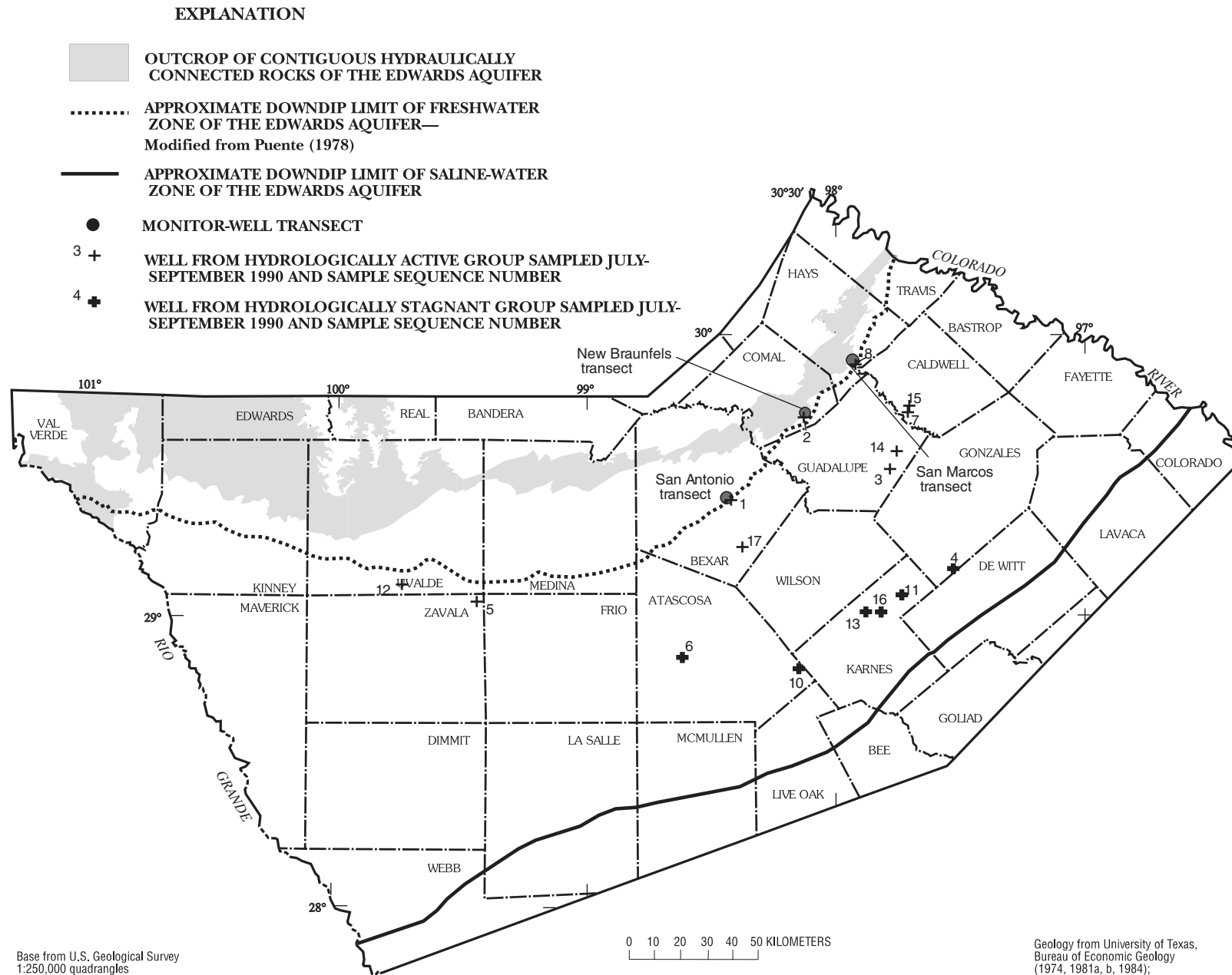


Figure 7. Location of sampled wells and monitor-well transects in San Antonio, New Braunfels, and San Marcos, Texas.

Table 1. Selected physical properties for samples from wells in the Edwards aquifer saline-water zone, south-central Texas, July-September 1990

[Samples from hydrologically stagnant group shown in bold. $\mu\text{S}/\text{cm}$, microsiemens per centimeter at 25 degrees Celsius; corrected pH, temperature- and pressured-adjusted pH computed by SOLMINEQ.88 (Kharaka and others, 1988); $^{\circ}\text{C}$, degrees Celsius; mg/L, milligrams per liter; —, no data]

Sequence number (fig. 7)	Well number	Date sampled	Land-surface altitude (meters above sea level)	Well depth (meters below land surface)	Specific conductance ($\mu\text{S}/\text{cm}$)		Field pH (standard units)	Corrected pH (standard units)	Field temperature ($^{\circ}\text{C}$)	Dissolved solids (mg/L)
					Field	Lab				
1	AY-68-37-523	07/30/90	189.3	358	5,800	5,710	7.3	7.12	27.0	4,310
2	DX-68-23-616	08/29/90	—	176	2,820	2,880	7.2	7.08	26.0	1,920
3	KX-67-26-9—	08/02/90	134.1	—	38,100	39,500	6.5	6.39	58.5	25,200
4	KR-67-52-6—	08/06/90	112.8	—	140,000	140,000	6.1	5.92	65.0	127,000
5	ZX-69-61-526	08/07/90	—	—	3,800	3,860	7.0	6.91	40.5	3,310
6	AL-78-12-1—	08/08/90	138.7	2,208	182,000	185,000	5.8	5.45	38.0	203,000
7	BU-67-19-4—	08/09/90	140.2	661	20,700	21,000	6.7	6.58	53.5	13,100
8	LR-67-01-812	08/13/90	—	165	13,500	14,500	6.8	6.59	25.5	9,550
10	AL-78-15-6—	08/17/90	—	—	116,000	191,000	5.6	5.44	45.0	232,000
11	PZ-67-58-6—	08/21/90	128.0	3,374	111,000	158,000	6.2	5.90	79.0	155,000
12	YP-69-59-101	08/22/90	—	502	2,920	3,510	6.9	6.78	36.0	3,160
13	PZ-67-57-9—	08/24/90	—	—	112,000	199,000	6.0	5.71	43.5	231,000
14	KX-67-26-3—	09/05/90	153.0	—	37,200	38,200	6.4	6.29	57.0	24,600
15	BU-67-19-1—	09/06/90	—	—	19,900	21,700	6.7	6.55	47.5	13,100
16	PZ-67-58-7—	09/08/90	96.9	—	—	186,000	5.9	5.61	40.0	214,000
17	AY-68-45-901	09/10/90	155.7	890	4,390	5,470	7.0	6.85	36.0	4,360

Table 2. Alkalinity and concentrations of major dissolved ions and dissolved silica for samples from wells in the Edwards aquifer saline-water zone, south-central Texas, July–September 1990

[Samples from hydrologically stagnant group shown in bold. In milligrams per liter; <, less than]

Sequence number (fig. 7)	Well number	Dissolved calcium	Dissolved magnesium	Dissolved sodium	Dissolved potassium	Alkalinity	Dissolved chloride	Dissolved sulfate	Dissolved sulfide	Dissolved fluoride	Dissolved silica
1	AY-68-37-523	550	210	470	25	250	970	1,800	<0.5	2.7	19
2	DX-68-23-616	150	100	300	21	250	510	520	7.5	2.5	13
3	KX-67-26-9—	1,900	580	6,500	130	410	¹ 14,000	1,700	48	5.1	26
4	KR-67-52-6—	13,000	1,100	32,000	1,100	270	76,000	<1.0	95	25	110
5	ZX-69-61-526	690	100	200	11	200	360	1,700	22	2.6	19
6	AL-78-12-1—	18,000	2,900	51,000	3,200	340	¹ 125,000	120	500	9.4	28
7	BU-67-19-4—	840	350	3,300	160	700	6,800	710	390	4.1	24
8	LR-67-01-812	930	440	1,800	80	390	3,600	2,300	45	1.3	15
10	AL-78-15-6—	17,000	1,600	63,000	5,800	180	¹ 140,000	2.4	58	3.0	54
11	PZ-67-58-6—	14,000	1,300	40,000	1,300	220	95,000	2.5	.8	27	81
12	YP-69-59-101	640	66	170	14	180	240	1,800	5.9	1.8	16
13	PZ-67-57-9—	20,000	1,600	61,000	4,500	220	¹ 140,000	4.5	50	5.1	61
14	KX-67-26-3—	1,600	540	6,700	270	420	14,000	770	320	<.10	26
15	BU-67-19-1—	840	400	3,400	150	490	6,700	980	190	5.9	21
16	PZ-67-58-7—	18,000	1,500	57,000	3,400	120	¹ 130,000	5.6	14	38	60
17	AY-68-45-901	610	210	400	20	240	790	2,000	51	2.6	26

¹ Estimated from cation-anion balance.

Table 3. Summary of mineral saturation indices computed by SOLMINEQ.88 (Kharaka and others, 1988) for samples from wells in the Edwards aquifer saline-water zone, south-central Texas, July–September 1990

[Mineral saturation index = \log_{10} (ion activity product/equilibrium constant) at estimated temperature; estimated temperature for in-place conditions. Samples from hydrologically stagnant group shown in bold. °C, degrees Celsius; a, extremely undersaturated]

Sequence number (fig. 7)	Well number	Mineral saturation index											Estimated temperature (°C)
		Anhydrite	Calcite	Celestite	Dolomite	Fluorite	Gypsum	Magnesite	Quartz	Sepiolite	Hematite	Pyrrhotite	
1	AY-68-37-523	-0.04	0.66	-0.31	2.56	-0.01	0.04	0.35	0.12	-2.11	0.02	-0.55	55
2	DX-68-23-616	-1.17	.16	-.53	1.64	-.18	-.99	-.02	.11	-5.53	-2.81	.32	42
3	KX-67-26-9—	.13	.37	-.20	2.17	.02	.02	.08	-.02	-4.12	-2.21	.75	80
4	KR-67-52-6—	-3.12	.56	-3.36	2.75	.10	-4.29	-.80	-.14	.65	-1.66	.44	175
5	ZX-69-61-526	-.03	.38	-.28	1.48	.29	.11	-.41	.20	-5.73	-2.56	.82	47
6	AL-78-12-1—	-.42	-.04	-.74	1.50	-.63	-1.04	-.62	-.22	-5.70	-3.55	.96	121
7	BU-67-19-4—	-.27	.69	-.34	2.98	-.29	-.42	.54	-.12	-3.21	-2.01	1.74	84
8	LR-67-01-812	.15	.41	-.24	2.27	-.90	.15	.25	-.09	-5.26	-2.98	.57	65
10	AL-78-15-6—	-1.83	.09	-1.88	1.73	-1.54	-2.80	-.93	-.18	-4.07	a	-.21	150
11	PZ-67-58-6—	-1.88	.48	-1.95	2.53	.34	-2.85	-.60	-.10	-.04	-1.25	-1.53	155
12	YP-69-59-101	.16	.43	-.27	1.61	-.15	.20	-.40	-.04	-6.62	-1.38	.40	62
13	PZ-67-57-9—	-1.49	.40	-1.76	2.38	-1.28	-2.60	-.84	-.25	-1.29	-2.12	.01	165
14	KX-67-26-3—	-.24	.36	-.54	2.23	-4.12	-.37	.13	-.06	-4.84	-2.69	1.44	83
15	BU-67-19-1—	-.33	.44	-.37	2.42	.11	-.36	.32	-.06	-4.27	-2.45	1.43	73
16	PZ-67-58-7—	-1.42	.04	-1.70	1.68	.48	-2.50	-1.16	-.26	-2.35	-2.19	-.66	164
17	AY-68-45-901	.01	.41	-.33	2.05	-.10	.08	.08	.20	-3.29	-2.79	.82	58

Uncertainties in Equilibrium Species Distribution

Large uncertainties of the computed equilibrium species distribution results are related mostly to the accuracy and precision of the pH and temperature measurements of 1,000- to 3,500-m-deep wells. The estimated in-place temperatures were used for the SI computations. The difference between the temperatures during pH measurements and the corrected in-place temperatures, on the basis of cation geothermometers, required recomputing pH on the basis of mass balance. Generally, the pH for the corrected in-place temperature was less than 0.3 standard unit different from the field-measured pH (table 1), but it was sufficient to cause substantial differences in some SIs. In all cases, the temperature-corrected pH was lower at the higher temperature. Therefore, the effect on the pH-dependent SI, such as for carbonate- and magnesium-containing minerals, was to decrease the SI by as much as 0.3. All pH-corrected SIs for calcite were approximately zero so the pH adjustment affected these SIs the most. Dolomite SIs were 1.5 or greater in almost all case; thus, the pH correction had little effect (table 3).

Pressures were not measured in the field because pressure measured at land surface would not be representative of pressure in the aquifer. Pressures estimated on the basis of average hydrostatic gradient and fluid density range from 12 to 50 MPa (120 to 500 bars).

The presence of hydrocarbons, including gases at or above the saturation partial pressure for in-place conditions, can affect geochemistry substantially. SOLMINEQ.88 can be used to assess the effect of these hydrocarbons, but the small amount of hydrocarbon data collected for this study did not support such a detailed analysis. Separate phases of hydrocarbons can move in directions other than that of hydraulic gradient because of buoyancy. Movement of a gas phase could carry off hydrogen sulfide and carbon dioxide; both are weak acids that can substantially affect the chemical environment in the subsurface.

Heterogeneous reactions, those involving mass transfer among phases or multiple states of matter, are more complicated than purely aqueous-phase (dissolved species) reactions. High pressure affects gas-phase reactions substantially more than it affects liquid-phase reactions because of the high molar volume of gases with respect to condensed phases.

A gas phase in the Edwards aquifer at sampled wells is difficult to determine. Much of the gas recovered in a sample at land surface could have been

dissolved in the aquifer water at high pressure. Furthermore, the condensation of gases to liquid (including condensate from wells producing natural gas) could greatly affect concentrations, especially with respect to condensation of water vapor. Hydrogen sulfide and carbon dioxide compose the bulk of the dissolved gases; methane and nitrogen are present in minor and variable amounts.

Temperature and Hydrogen Activity

Estimated in-place temperatures of the samples collected for this study indicate an increase with depth and (or) distance from the downdip limit of freshwater (fig. 8). Estimated in-place temperatures are less than 85 °C for the hydrologically active group of samples and 121 to 175 °C for the hydrologically stagnant group of samples. The Stuart City Formation is the deepest geologic unit and is the downdip limit of the Edwards aquifer, so a direct relation between temperature and proximity to the Stuart City Formation is consistent. Most temperatures in parts of the saline-water zone are at or slightly above the temperature expected for the natural geothermal gradient (Woodruff and Foley, 1985). The reason for the higher than expected temperatures is unknown, but Woodruff and Foley (1985) hypothesized that upward movement of fluids along faults from beneath the Cretaceous sediments in the area might explain the temperature anomalies. On the basis of chemistry of water samples from the Edwards aquifer saline-water zone, Land and Prezbindowski (1981, 1985) and Clement and Sharp (1988) also inferred that hot brines from beneath the aquifer move upward into the Edwards aquifer continuously or episodically.

The pH of water samples from the saline-water zone decreases with increasing distance from the downdip limit of freshwater. The pH becomes much more acidic with increasing depth, dissolved solids concentration (fig. 9), temperature, and pressure. (pH shown in fig. 9 are temperature-adjusted pH computed by SOLMINEQ.88.) The temperature- and pressure-adjusted pH ranges from 6.29 to 7.12 for the hydraulically active group of samples and from 5.44 to 5.92 for the hydraulically stagnant group of samples (table 1). At least part of the decrease in pH downdip is caused by the increasing temperature. The pH of freshwater decreases from 7.0 to 5.8 when heated from 25 to 150 °C (Hanor, 1979, p. 149). Many other factors, including sulfide oxidation, could cause the increase in

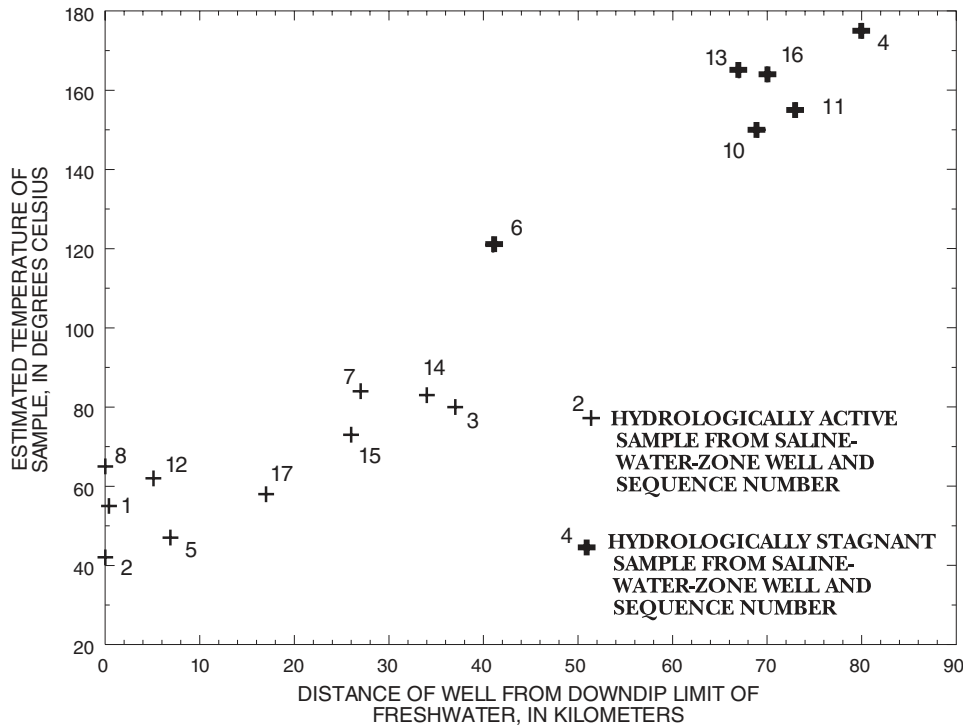


Figure 8. Relation between estimated in-place temperature of ground-water samples and distance of well from the downdip limit of freshwater in the Edwards aquifer, south-central Texas.

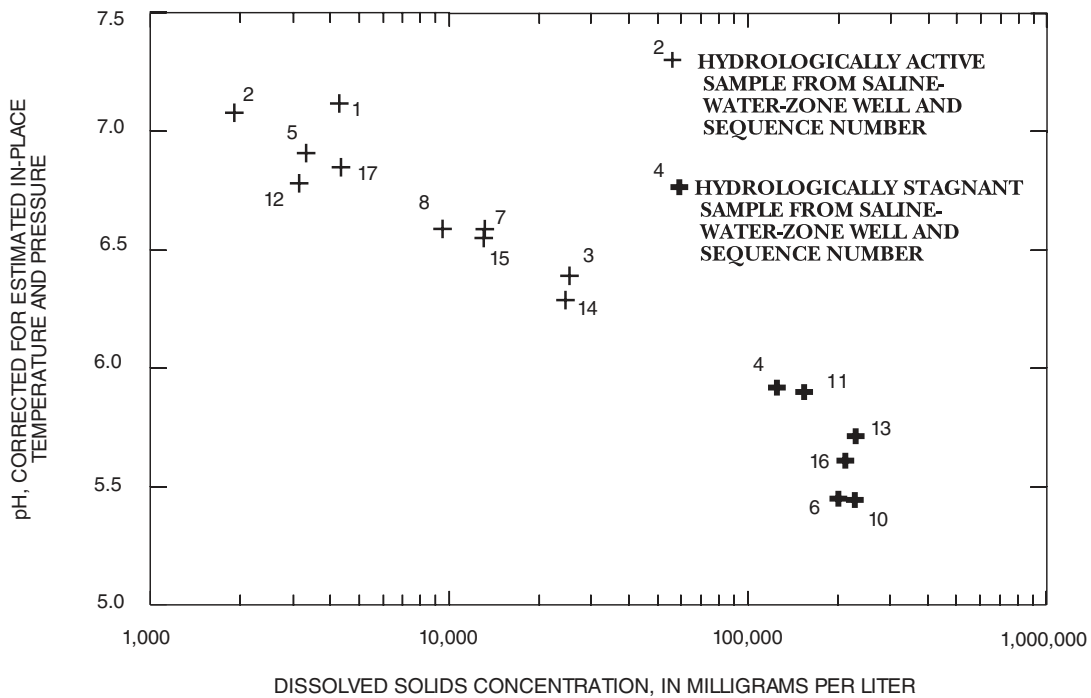


Figure 9. Relation between corrected pH and dissolved solids concentration in ground-water samples from the Edwards aquifer saline-water zone, south-central Texas.

acidity with increasing distance from the down-dip limit of freshwater, but most of the increase in acidity is caused by high temperatures.

Dissolved Constituents

Dissolved Solids

The dissolved solids concentrations used in this report from the TP file are defined as the sum of the concentrations of ions in solution determined for each complete water sample. Each sample analysis comprised determinations for all major ions: calcium, magnesium, sodium, potassium, bicarbonate, chloride, and sulfate. Additionally, the cation-anion balance, in equivalents, was 0.00 ± 0.10 . Results for dissolved silica were not available for many wells. (Most dissolved solids concentrations are 10,000 mg/L or greater, and dissolved silica concentrations generally are less than 100 mg/L; thus, the error associated with not including dissolved silica concentrations in the sum of dissolved solids is considered inconsequential.) The dissolved solids concentrations of samples collected from the 16 saline-water-zone wells during this study are defined similarly, but the sums all include dissolved silica; the cation-anion balance, in equivalents, generally is 0.00 ± 0.05 . Dissolved solids concentrations range from 1,920 to 25,200 mg/L for the hydraulically active group of samples and from 127,000 to 232,000 mg/L for the hydraulically stagnant group of samples (table 1).

Many wells represented by data in the TP file were sampled and analyzed more than once and at different times over a period of years, and large changes in dissolved solids concentrations between samples at individual wells are apparent. Almost all the changes are increases in dissolved solids concentration over time.

A comparison of salt-normative mineral assemblages (salt norms) of ground-water samples collected over time can help identify what kinds of changes occurred among the well-water samples that varied in composition over time. The salt norm is the quantitative ideal equilibrium assemblage of minerals that would crystallize if the water evaporated to dryness at 25 °C and 0.1-MPa pressure under atmospheric partial pressure of CO₂ gas. The model SNORM (Bodine and Jones, 1986) computes the salt norm for a given water chemistry on the basis of ionic proportions of the water-sample analyses. If two water samples have similar dissolved solids concentrations but substantially different

ionic proportions, the salt norms of the two samples would be substantially different. Likewise, if the dissolved solids concentrations of two samples were vastly different, yet ionic proportions were similar, the salt norms computed for the two samples would be similar.

The salt norms were computed for selected water-sample analyses from the TP file that indicate changes in dissolved solids concentration at particular wells over time (table 4). Differences of 2 to about 5 percent in salt-norm anhydrous weights are inconsequential unless the difference is sufficient to change the relative order of the percentages (Bodine and Jones, 1986). Despite relatively large increases in dissolved solids concentration at several wells, the relative proportions of the major ions in all samples did not change substantially; therefore, the order of the weight percentages in the salt norms are similar. The intrawell similarity of the salt norms indicates that the solute source for the wells did not change over the period represented by the sample data. The interwell similarity of the salt norms in table 4 indicates that the source of solutes is the same for all wells.

On the basis of salt-norm results, the most likely explanation for the lower dissolved solids concentrations in the earlier samples of the TP file is that the water collected in the wells at the earliest samplings was from near the top of the Edwards aquifer in a zone where salinity was much lower than in most of the aquifer below. Such a top-of-aquifer zone of dilute water, yet similar in ionic proportions to deeper water, is located in the vicinity of the San Antonio freshwater/saline-water transect wells (Groschen, 1994).

Another explanation for the lower concentrations in the earlier samples is that they were affected by dilution from water condensation during sampling (Gautier and others, 1985). A substantial amount of hot water vapor in the gas phase of the fluid in the sampled well was likely if (1) a substantial gas phase existed in the hydrocarbon-producing zone, or (2) dissolved gas exsolved when fluid was withdrawn. As the fluid moved up the well casing and cooled, much of the water vapor would have condensed and diluted the water exiting the well casing at land surface. As the gas phase in the Edwards aquifer was removed and pressure in the producing zone was reduced as a result of fluid withdrawals, there would be less water vapor to condense; therefore, the later samples would be more saline, but would retain the relative ionic proportions of the earliest sample. Without more information about the production history and pressure decrease with time after the initial

Table 4. Dissolved solids concentrations and anhydrous weight percentages of computed salt-normative mineral assemblages for samples from selected wells in the Edwards aquifer saline-water zone, south-central Texas, collected over various time periods

[Well identifier from Taylor (1975) and Pettijohn (1986). mg/L, milligrams per liter; —, less than 1 percent; sum of percentages may not add up to 100 because of rounding]

Well identifier and county	Date sampled	Dissolved solids (mg/L)	Computed salt-normative mineral assemblage (weight percent)				
			Halite	Antarcticite	Tachyhydrite	Anhydrite	Dolomite
4201301136_344518 Atascosa	1942	42,000	76	17	3	2	1
	1942	176,000	72	23	5	—	—
	1942	209,000	71	25	4	—	—
4201301138_344518 Atascosa	1942	63,400	71	24	4	—	—
	1942	96,200	70	23	5	—	—
	1942	168,000	72	22	6	—	—
4201301192_344518 Atascosa	1943	19,100	79	8	4	7	2
	1943	30,100	73	18	3	3	2
	1945	196,000	79	15	6	—	—
4201301197_344518 Atascosa	1943	30,400	77	14	5	2	1
	1945	176,000	70	26	5	—	—
	1965	180,000	71	21	8	—	—
4201301909_344518 Atascosa	1945	81,500	74	14	11	—	—
	1956	186,000	74	20	6	—	—
4201302151_134116 Atascosa	1944	33,200	88	7	2	1	2
	1945	170,000	91	6	2	—	—
4205504538_626456 Caldwell	1947	8,300	78	7	9	1	5
	1947	21,200	78	10	11	1	—
4216301531_999999 Frio	1964	148,000	72	20	6	1	—
	1964	185,000	71	21	7	—	—
	1964	196,000	71	21	7	—	—
	1964	199,000	71	21	8	—	—
4218700995_181209 Guadalupe	1930	27,600	73	6	11	8	2
	1965	25,300	72	9	12	6	2
4225500084_001609 Karnes	1959	207,000	73	22	4	—	—
	1959	230,000	72	24	3	—	—
	1959	231,000	72	22	5	—	—

Table 4. Dissolved solids concentrations and anhydrous weight percentages of computed salt-normative mineral assemblages for samples from selected wells in the Edwards aquifer saline-water zone, south-central Texas, collected over various time periods—Continued

Well identifier and county	Date sampled	Dissolved solids (mg/L)	Computed salt-normative mineral assemblage (weight percent)				
			Halite	Antarctite	Tachyhydrite	Anhydrite	Dolomite
4225500100_551637 Karnes	1961	165,000	63	18	18	—	—
	1961	170,000	71	25	4	—	—
	1961	171,000	71	24	4	—	—
	1966	180,000	71	23	5	—	—
4225500103_551637 Karnes	1960	90,700	73	20	6	1	—
	1966	110,000	75	21	4	—	—
4225500105_013355 Karnes	1960	182,000	65	29	6	—	—
	1960	192,000	67	27	6	—	—
	1966	177,000	72	23	5	—	—
4225500130_013255 Karnes	1960	98,300	80	15	5	—	—
	1960	108,000	78	16	5	—	—
4225500152_393161 Karnes	1962	184,000	68	24	8	—	—
	1966	211,000	70	24	5	—	—
	1966	215,000	71	23	5	—	—
4225500181_551637 Karnes	1961	120,000	74	19	6	—	—
	1966	7,400	75	17	6	—	1
4225500723_017506 Karnes	1961	98,400	79	18	2	—	—
	1961	98,400	79	19	2	—	—
	1961	157,000	72	24	4	—	—

construction of the wells, this explanation for the observed increases in salinity over time remains speculative.

Dissolved solids concentrations generally increase from the downdip limit of freshwater toward the downdip limit of the saline-water zone. This geographic relation was examined by plotting the dissolved solids concentrations of the 16 samples collected for this study against the shortest distance from the downdip limit of the freshwater to the sampled well (fig. 10). Excluding sample 6, the data in figure 10 generally form two distinct groups on the basis of well location in the saline-water zone. One group comprises samples from

shallow wells within the hydrologically active group. The other group comprises samples from deep wells in the hydrologically stagnant group. The data of the two groups appear to form almost a straight line from least salinity to greatest salinity. This pattern indicates a relatively monotonic increase in salinity from updip to downdip.

If concentrated brines were entering the saline-water zone of the Edwards aquifer along faults, then the expected distribution of salinity likely would not be monotonic. The concentrations would be expected to be largest near (or downgradient from) faults that are conducive to upward recharge to the aquifer from deeper

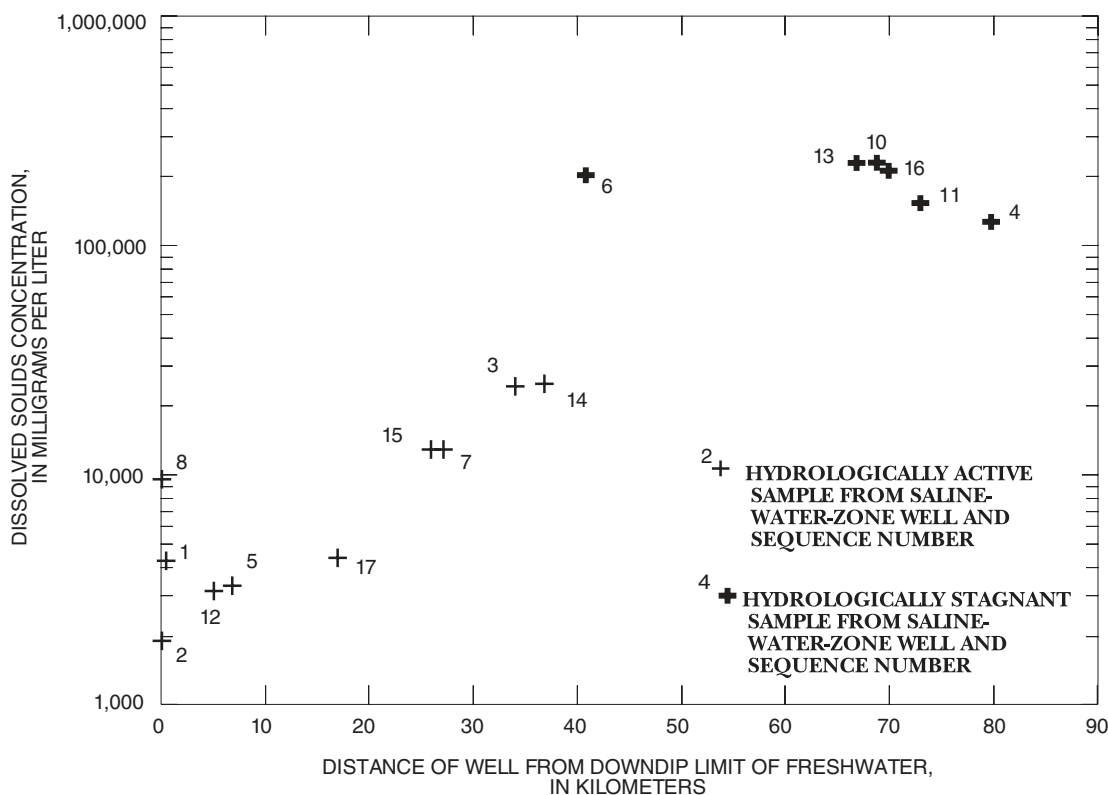


Figure 10. Relation between dissolved solids concentration in ground-water samples from the saline-water zone and distance of the well from the downdip limit of freshwater in the Edwards aquifer, south-central Texas.

brine sources. The shallow oil fields generally produced more liquid hydrocarbons than the deeper fields, and considerable quantities of saline water were withdrawn with the hydrocarbons from the shallow fields (Cook, 1979). Upfault flow of highly saline brines would be manifest at these shallow fields, in part because the fields are nearly always formed by large fault displacements. Large fluid withdrawals from hydrocarbon-producing wells would tend to increase the gradient from the hypothetical deep brine sources (or other sources) to the Edwards aquifer, increasing the possibility that saline brine would be drawn into the Edwards aquifer along faults within or bounding a field. Given the uniformity of the downdip increase in dissolved solids concentration indicated in figure 10, recharge along faults from deep brine sources is unlikely.

A younger overlying source of chloride-rich brine is unlikely because of the thick sequence of poorly permeable Upper Cretaceous and Tertiary sediments between the top of the Edwards aquifer and any possible source aquifer. Nevertheless, two conditions could enable downward migration of brine from an overlying source. The first condition is that pockets of geopres-

sured sediments might be present within the Tertiary sediments; the second is that faults potentially capable of allowing deeper fluid up into the Edwards aquifer (Land and Prezbindowski, 1981, 1985; Woodruff and Foley, 1985; Clement and Sharp, 1988) might also be capable of carrying fluids downward from overlying geopressed sediments.

Chloride

Dissolved chloride concentrations in water from sampled wells range from 240 to 140,000 mg/L (table 2); 240 to 14,000 mg/L in hydraulically active samples and 76,000 to 140,000 mg/L in hydraulically stagnant samples. The largest chloride concentrations, similar to dissolved solids concentrations, generally are at the wells farthest downdip in samples from the hydrologically stagnant group, near the Stuart City Formation (fig. 3). In small areas updip from the Stuart City Formation and generally isolated within certain oil fields, concentrations are as large as those at the downdip edge of the aquifer. The local chloride highs could be related to the tendency of some wells to yield water with

increasing dissolved solids concentrations over time. The McKnight and possibly West Nueces and Salmon Peak Formations in the western part of the area contain primary deposits of rock salt (halite) (Getzender, 1930). The total mass of halite originally deposited in the aquifer rocks is unknown; therefore, it is unclear whether the aquifer matrix could account for all the dissolved sodium and chloride in the saline-water zone.

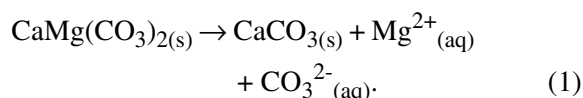
Calcium and Magnesium

Dissolved calcium concentrations in water from sampled wells range from 150 to 20,000 mg/L; 150 to 1,900 mg/L in the hydraulically active samples and 13,000 to 20,000 mg/L in the hydraulically stagnant samples. Dissolved magnesium concentrations range from 66 to 2,900 mg/L (table 2); 66 to 580 mg/L in the hydraulically active samples and 1,100 to 2,900 mg/L in the hydraulically stagnant samples. Rose (1972) reported that the relative amount of dolomite was greatest along the crest of the San Marcos platform (fig. 3). Fisher and Rodda (1969) and Rose (1972) concluded that the dolomitization of the Edwards aquifer matrix rocks occurred during the Cretaceous period. The relative abundance of dolomite in the aquifer matrix might explain the spatial variation in dissolved calcium and magnesium concentrations. Winter (1961) reported some dolomite in the western part of the saline-water zone, about 10 to 20 percent of the combined thickness of the aquifer matrix. Near the Stuart City Formation, dissolved calcium concentrations in ground-water samples are relatively large with respect to dissolved magnesium concentrations. Bebout and Loucks (1974) found little evidence of dolomite in the Stuart City Formation. Therefore, assuming that the limestone of the Stuart City Formation originally was mostly low-magnesian calcite and that it had not changed substantially since burial (Prezbindowski, 1981), equilibration of the water with aquifer-matrix minerals accounts for the large dissolved calcium concentrations relative to dissolved magnesium concentrations in the sample data from the Stuart City Formation area.

All the 1990 water samples from the saline-water zone are supersaturated with respect to dolomite (fig. 11). The amount of apparent supersaturation probably is the result of errors in pH and temperature estimations and errors in the solubility product for dolomite at high temperatures, or perhaps the failure to account for magnesium-containing aqueous complexes. The greatest supersaturation of water samples with respect to

dolomite is from wells along the crest of the San Marcos platform (fig. 4). These wells are roughly in the area that contains the greatest amount of dolomite in the rocks (Rose, 1972). Water samples from wells in the area of greatest dolomite percentage are saturated with respect to magnesite; whereas samples from other wells are undersaturated. The SIs for dolomite and magnesite do not imply that either dolomite or magnesite is likely to precipitate but only indicate the state of supersaturation. Other factors, including the kinetics of precipitation, can control formation of these minerals.

The apparent supersaturation with respect to dolomite appears to be related directly to the relative amount of dolomite in the rocks. Dissolution of dolomite in the saline-water zone is the most probable reaction. At the calcite saturation-phase boundary, dissolution of dolomite would continue to the point of dolomite saturation. The phase most likely to precipitate because of the increased calcium and alkalinity (bicarbonate) from dolomite dissolution is magnesian calcite rather than dolomite (Morrow, 1982). The relative amount of calcium removed from solution by the precipitation of magnesian calcite would be greater than the amount of magnesium, thus increasing the relative amount of dissolved magnesium in solution. This process is described variously as incongruent dissolution of dolomite, dedolomitization, or calcite stabilization, and it increases the amount of dissolved magnesium relative to calcium. The net reaction can be written as follows:



Evidence for dedolomitization is common in the freshwater zone of the Edwards aquifer and diminishes with distance down dip from the freshwater zone into the saline-water zone (Mench-Ellis, 1985; Deike, 1990). Prezbindowski (1981) reported some evidence of dedolomitization in the deep saline-water zone, but only in areas that were exposed to surface weathering prior to deposition of the Georgetown Formation (Rose, 1972). Prezbindowski (1985) also concluded that most cementation (precipitation of calcite between sediment grains and other processes involving the precipitation of carbonate minerals) in the saline-water zone occurred long before deep burial.

The interwell similarity of salt norms for samples from selected wells indicates that the sources of solute were similar (table 4). The salt-norm minerals that change relative rank from one well to another are

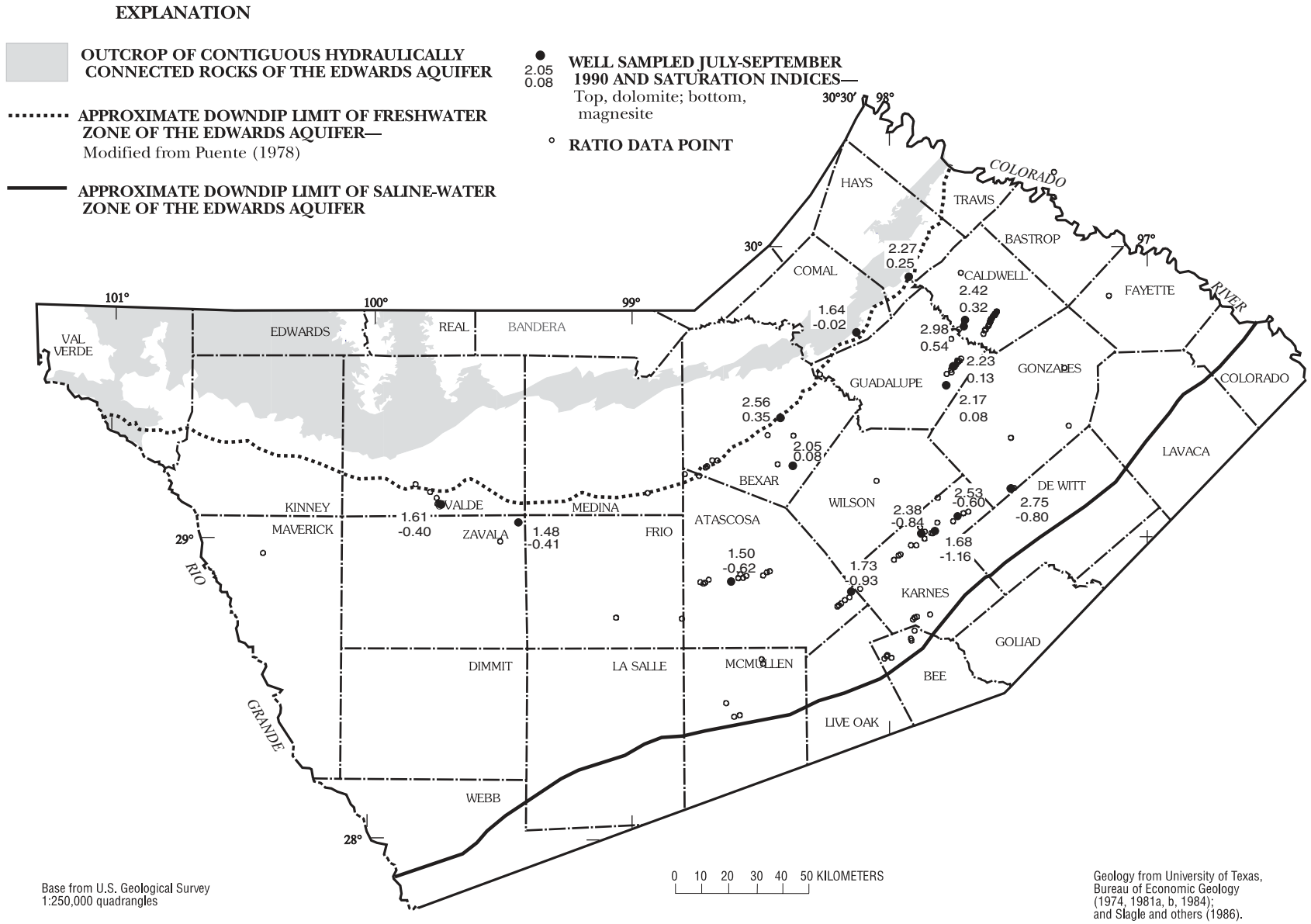


Figure 11. Mineral-saturation indices of dolomite and magnesite in ground-water samples from the Edwards aquifer saline-water zone, south-central Texas.

antarcticite and tachyhydrite. The proportions of these two minerals in the salt norm are a result of the relative proportions of calcium and magnesium dissolved in the water sample. The proportion of antarcticite to tachyhydrite is larger in the salt norms for all but two wells. Salt norms for wells 4205504538_626456 (Caldwell County) and 4218700995_181209 (Guadalupe County) have larger proportions of tachyhydrite to antarcticite (table 4). The greater proportion of tachyhydrite to antarcticite results from relatively more dissolved magnesium compared to dissolved calcium in water samples from the two wells than in samples from the other wells. Both wells are in the area where the Edwards aquifer matrix contains the highest percentage of dolomite and are relatively close to the downdip limit of freshwater (fig. 11). The salt norms indicate that the source of dissolved magnesium is likely the dolomite in the aquifer matrix.

An alternative explanation for the relatively low dissolved magnesium compared to dissolved calcium in the deep well samples is that high temperatures create conditions for precipitation of magnesium silicates. The SIs listed in table 3 indicate that sepiolite is at or near saturation in two well samples. The kinetics of magnesium-silicate precipitation from solution is poorly understood; therefore, the significance of magnesium-silicate precipitation in controlling the level of dissolved magnesium is unknown.

The ratio of magnesium to calcium in the saline-water zone appears to be determined by the amount of dolomite in the rocks and not by the flow of a magnesium-poor diagenetic or geothermal fluid into the aquifer. Dedolomitization has been a major process and is occurring because of the influence of fresh meteoric water in the saline-water zone (Deike, 1990).

Sulfur

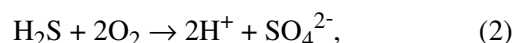
Dissolved, Gas Phase, and Nonaqueous Liquid Phase

Dissolved sulfate (SO_4^{2-}) is the predominant sulfur species in solution in normal oxygenated ground water (Pearson and Rightmire, 1980). In strongly reducing aqueous conditions, however, the dominant dissolved equilibrium sulfur species depends on the pH of the solution (Garrels and Christ, 1965, p. 213). At pH greater than 7.0, bisulfide ion predominates; at pH less than 7.0, hydrogen sulfide predominates. At pH of 7.0, the two species are at approximately equal concentrations. The corrected pH for all but two of the saline-water-zone samples (table 1) is less than 7.0; therefore,

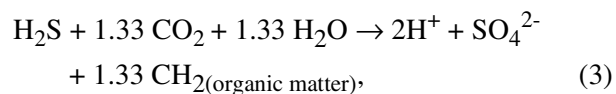
hydrogen sulfide predominates in those samples. In the following discussion, hydrogen sulfide is used to refer to the sum of reduced sulfur species, even though some bisulfide also is present in the sample.

Dissolved sulfate concentration is quite variable among the available analyses and appears to have little relation to other factors, including dissolved sulfide. The only trend apparent in the dissolved sulfate concentrations from the samples collected for this study and from the TP file is that sulfate concentrations in the saline-water zone tend to be largest near the downdip limit of freshwater. Dissolved sulfate concentrations range from <1.0 to 2,300 mg/L; 520 to 2,300 mg/L in the hydraulically active samples and less than 120 mg/L in the hydraulically stagnant samples. The simplest explanation is that oxygen or other oxidized species move with recharge water into the saline-water zone from the freshwater zone and, either directly or through bacterial mediation, oxidize hydrogen sulfide.

The SI for gypsum is the closest to saturation (nearly equal to zero) in water samples from within 40 km of the downdip limit of freshwater. Few sulfate concentrations are larger than would be expected for the saturation level of gypsum or anhydrite (CaSO_4); therefore, the sulfate concentration likely is limited by the solubility of gypsum or anhydrite. Gypsum and anhydrite, or evidence of gypsum and anhydrite in the aquifer rocks, was reported by Winter (1961), Tucker (1962), and Rose (1972). Oxidation of hydrogen sulfide to sulfate by the net reaction



or by biological mediation



in the saline-water zone near the downdip limit of freshwater could result in the precipitation of gypsum. The release of hydrogen ions by the above reactions also would increase the dissolution of carbonate minerals. Some anhydrite or gypsum, usually 5 percent or less of the rock matrix, is indicated in mineral identification of rocks from the saline-water zone (Winter, 1961; Rose, 1972; Mench-Ellis, 1985; Deike, 1990).

Deike (1990) concluded that dedolomitization caused by the mixing of Edwards aquifer freshwater with saline water near the downdip limit of freshwater was the dominant process responsible for developing the large secondary porosity and extremely high

transmissivity in the freshwater zone. Dedolomitization in this mixing zone could be driven by gypsum dissolution. If gypsum solubility controls the concentration of dissolved sulfate in the saline-water zone near the downdip limit of freshwater, and if gypsum is precipitating in this part of the saline-water zone, then gypsum precipitation might enhance further dedolomitization as freshwater moves into the saline-water zone. Other geochemical processes, such as oxidation of organic matter and reduction of sulfate by sulfide, make it difficult to evaluate the effect of specific processes.

Dissolved sulfide concentration is extremely variable in the saline-water zone (table 2). The most likely reason for the presence of sulfide in the saline-water zone is bacterial or thermochemical reduction of sulfate. Feely and Kulp (1957) demonstrated that bacterial reduction of sulfate from evaporite deposits is the major mechanism for the accumulation of elemental sulfur and reduced sulfur species in the areas around salt domes in the Gulf Coast region. Part of the South Texas Salt Basin, comprising Jurassic evaporite deposits, underlies the Edwards aquifer saline-water zone, and one salt dome pierces the Edwards aquifer (fig. 4) (Beckman and Williamson, 1990).

The salt domes in Texas, including the one that pierces the Edwards aquifer, have the same Jurassic (Louann Salt) source and similar overlying stratigraphy. Vertical flow of water similar to that proposed by Hanor (1987b) might occur near the salt domes in Texas. Salt-dome related brine thus could be a source of dissolved sulfate, chloride, and sodium to the Edwards aquifer saline-water zone. Sulfate dissolved from the evaporite deposits and the presence of easily decomposed hydrocarbons or other organic compounds are sufficient for the sulfate-reduction process described in Feely and Kulp (1957). The substantial variability in sulfide concentrations might be caused by a limited or patchy distribution of bacteria, evaporite minerals, or hydrocarbons.

Movement of gas-phase hydrogen sulfide also could be a cause of variability of dissolved hydrogen sulfide in the saline-water zone. If hydrogen sulfide and other gases exceed the pressure solubility for the local physical environment, they can exsolve from solution and move as a separate gas phase. Buoyancy of the gas would cause it to move directly updip, following the slope of the overlying confining unit, even though the water might be relatively stagnant or might be flowing normal to the dip (Dahlberg, 1982). Many of the oil fields contained substantial gas pockets (Rose, 1984).

Movement of gas-phase hydrogen sulfide might be an important process in the Edwards aquifer. As hydrogen sulfide gas moved updip, it would mix with dissolved oxygen or other oxidizing compounds, such as sulfate ions, and would oxidize, creating sulfuric acid in the process (eq. 2). Hill (1990) concluded that the oxidation of hydrogen sulfide gas seeping upward into shallow oxygenated ground water created the Carlsbad and Lechuguilla Caverns in New Mexico. Hydrogen sulfide oxidation near the downdip limit of freshwater could be a major process for development of the large transmissivity of the freshwater zone in the Edwards aquifer, and it also would help explain the large dissolved sulfate concentration in the hydraulically active regime of the saline-water zone.

Movement of a separate nonaqueous liquid phase also could help create the variability in sulfide distribution. The solubility in ground water of the nonaqueous liquid-phase organic compounds is likely to be much lower than the gas-phase solubility, so movement of a separate liquid phase orthogonal or counter to the flow of water is possible. This factor has been used to explain the location and development of the oil fields in the Edwards aquifer saline-water zone (Moredock and Van Siclen, 1964) and the occasional accumulation of oil in freshwater wells near the downdip limit of freshwater. The nonaqueous liquid phase might contain large amounts of dissolved hydrogen sulfide or other reduced sulfur species.

Stable Isotopes

The relative amount of ^{34}S , a stable isotope of sulfur, commonly is useful to determine the sources of sulfur species in water and the reactions that involve particular species (Pearson and Rightmire, 1980). Rightmire and others (1974) and Rye and others (1981) used isotope composition of dissolved sulfur species in water to determine that the sulfate in the Edwards aquifer freshwater zone is from a distant, wind-borne Permian source and is very different from the sulfate and sulfide of the saline-water zone. Rye and others (1981) also speculated that oxidation of hydrogen sulfide was occurring in the saline-water zone near the downdip limit of freshwater. Rye and others (1981) reported that the isotope fractionation between dissolved sulfate and sulfide was much lower than expected for equilibrium fractionation; they concluded that this resulted from large concentrations of organic matter and high temperatures in the saline-water zone

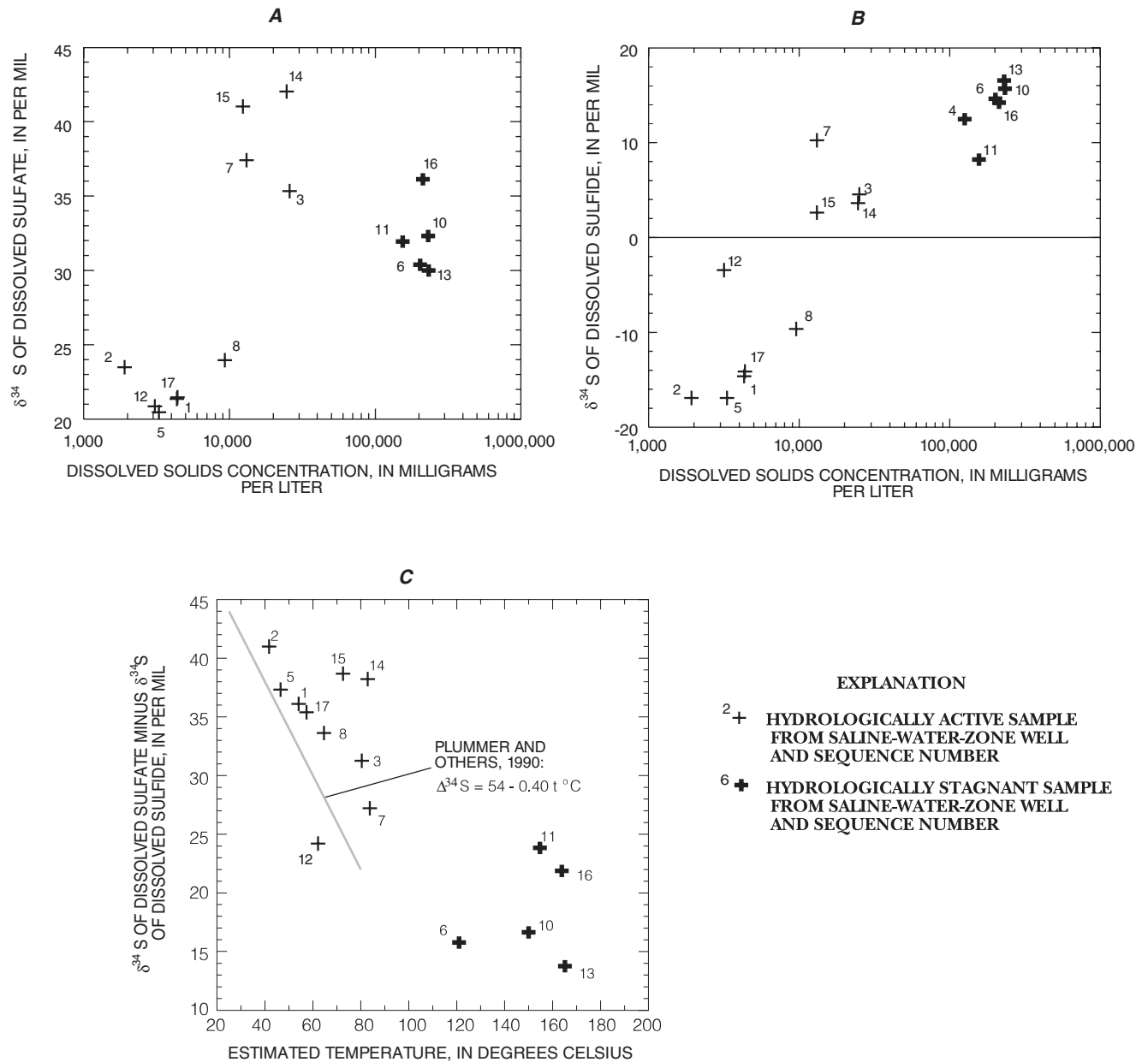


Figure 12. Relations between (A) del sulfur-34 ($\delta^{34}\text{S}$) of dissolved sulfate and dissolved solids concentration, (B) $\delta^{34}\text{S}$ of dissolved sulfide and dissolved solids concentration, and (C) $\delta^{34}\text{S}$ of dissolved sulfate minus $\delta^{34}\text{S}$ of dissolved sulfide and estimated temperature in ground-water samples from the Edwards aquifer saline-water zone, south-central Texas.

that caused the bacteria-mediated reaction to proceed too quickly for isotopic equilibrium to be attained.

Several graphs of the stable-isotope ratios of ^{34}S to sulfur-32 (^{32}S), $\delta^{34}\text{S}$, are shown in figure 12. The notation $\delta^{34}\text{S}$ expresses the ratio of ^{34}S to ^{32}S as referenced to Canyon Diablo Troilite (CDT). Figure 12A shows the relation of $\delta^{34}\text{S}$ of dissolved sulfate to dissolved solids concentration; figure 12B shows the rela-

tion of $\delta^{34}\text{S}$ of dissolved sulfide to dissolved solids concentration; and figure 12C shows the relation of the difference between $\delta^{34}\text{S}$ of sulfate and $\delta^{34}\text{S}$ of sulfide ($\Delta\delta^{34}\text{S}$) to estimated subsurface temperature. The two sets of $\delta^{34}\text{S}$ ratios also are plotted on a map in figure 13. The $\delta^{34}\text{S}$ values generally are close to those reported by Rye and others (1981), but the $\delta^{34}\text{S}$ of dissolved sulfate for the shallow oil-field wells (3, 7, 14, and 15) are

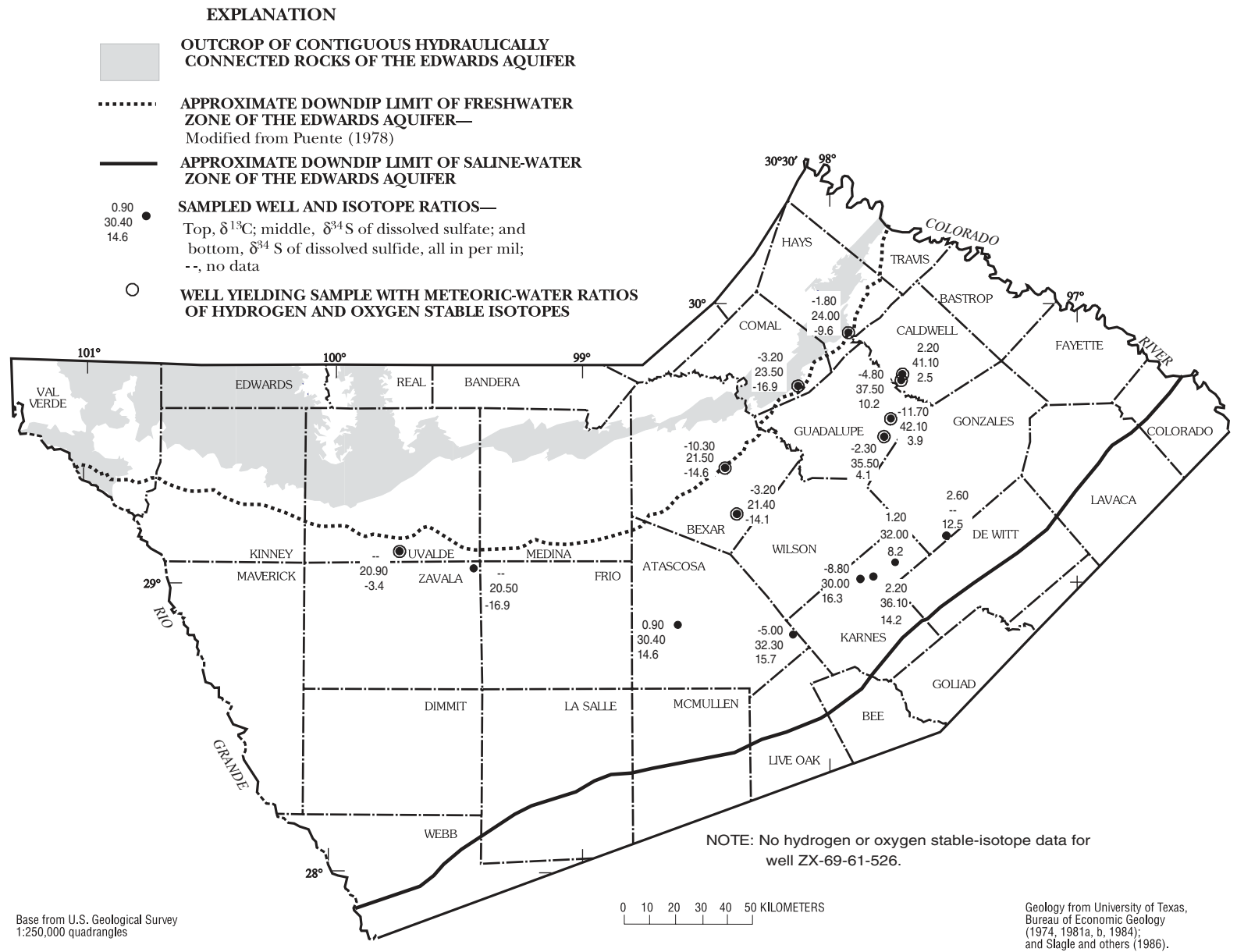


Figure 13. Distribution of del carbon-13 ($\delta^{13}\text{C}$) of dissolved inorganic carbon and del sulfur-34 ($\delta^{34}\text{S}$) of dissolved sulfate and sulfide in groundwater samples, and location of wells that produce water with meteoric del deuterium (δD) and del oxygen-18 ($\delta^{18}\text{O}$) in the Edwards aquifer saline-water zone, south-central Texas.

much greater (more enriched) than any reported by Rye and others (1981).

The data plotted in figures 12A and 12B fall into three subgroups on the basis of the relative differences in ^{34}S composition. The first subgroup comprises the least saline samples—the transition group (samples 1, 2, 5, 8, 12, and 17). These samples are slightly enriched in ^{34}S of dissolved sulfate and relatively depleted in ^{34}S of dissolved sulfide. The second subgroup comprises the samples from shallow oil and gas wells (samples 3, 7, 14, and 15). These samples are enriched in ^{34}S of dissolved sulfate and sulfide. The final sulfur isotope subgroup comprises samples from the hydrologically stagnant group (samples 4, 6, 10, 11, 13, and 16). These samples are enriched in ^{34}S of dissolved sulfide and enriched in ^{34}S of dissolved sulfate relative to transition-group samples.

In figure 12A, all the samples are enriched in ^{34}S of dissolved sulfate with respect to CDT. The most saline samples are intermediate in $\delta^{34}\text{S}$ between the transition-group samples and the shallow oil-field samples. If Jurassic or Cretaceous evaporite was the sulfate source and no other reactions were affecting isotope fractionation, the sulfate $\delta^{34}\text{S}$ should range from 15 to 17 per mil (Claypool and others, 1980). In fact, the enriched ^{34}S of sulfate is greater than any reported for natural evaporite deposits. Rye and others (1981) concluded that the $\delta^{34}\text{S}$ of sulfate in the saline-water zone was too large to be derived directly from either Jurassic or Cretaceous deposits.

A general trend can be seen in the data plotted in figure 12B—increasing enrichment in ^{34}S of dissolved sulfide from least salinity to greatest salinity. The transition-group samples show negative $\delta^{34}\text{S}$ of sulfide—depleted with respect to CDT and with respect to the more saline samples. The $\delta^{34}\text{S}$ of dissolved sulfide for the oil- and gas-field samples is enriched in ^{34}S with respect to CDT and the transition-group samples. The $\delta^{34}\text{S}$ of dissolved sulfide for the hydrologically stagnant samples is enriched in ^{34}S with respect to CDT and is enriched in ^{34}S with respect to hydrologically active samples, except for sample 7.

Sulfate reduction by biological and (or) thermochemical means must be occurring in the saline-water zone of the aquifer. The sulfate $\delta^{34}\text{S}$ reflects the remaining sulfate after incomplete reduction to sulfide. The amount of fractionation, and therefore the isotope composition of the product hydrogen sulfide and the remaining sulfate, is related to the temperature where the reduction of sulfate occurred. The sulfide produced

should be depleted in ^{34}S with respect to the original sulfate isotope composition.

Reduction results in the residual sulfate being slightly enriched in ^{34}S (fig. 12A) and the produced sulfide being depleted in ^{34}S (fig. 12B). The $\Delta^{34}\text{S}$ (fig. 12C) is the difference between the $\delta^{34}\text{S}$ of dissolved sulfate and of dissolved sulfide. H_2S oxidation reactions do not appear to substantially affect the $\delta^{34}\text{S}$ of the products or residue (Krouse, 1980); therefore, the fractionation between the two dissolved species reflects either sulfate reduction, movement of hydrogen sulfide away from the reaction site after sulfate reduction, or both processes. Using data derived, in part, from the Edwards aquifer, Plummer and others (1990, p. 1,993) developed an equation for the relation of $\Delta^{34}\text{S}$ to temperature:

$$\Delta^{34}\text{S} = 54 - 0.40 t, \quad (4)$$

where t is temperature in degrees Celsius, and t is about 20 to 80 °C. Data from the 11 hydrologically active samples (estimated temperatures of 42 to 84 °C) are similar to, but generally greater than, the relation of Plummer and others (1990).

Carbon

Dissolved

The major organic and inorganic dissolved carbon species for the 16 well-water samples collected during July–September 1990 are listed in table 5. The distributions of the dissolved carbon species are highly variable and do not indicate trends. Variability in the carbon species concentrations was expected, owing to the distribution of oil and gas fields in the saline-water zone of the Edwards aquifer. Dissolved inorganic carbon does not appear to be related to the concentration of dissolved organic carbon in the water sample. The concentrations of dissolved organic carbon in the samples generally are small with respect to the concentrations of inorganic carbon. The bicarbonate concentrations, assumed to be the main component of alkalinity as reported in the TP file, are not related to the location of oil fields or distance from the downdip limit of freshwater.

Several researchers (Carothers and Kharaka, 1978a, b; Lundegard and Land, 1986; Fisher, 1987) have reported that low-molecular weight aliphatic acids commonly comprise a substantial proportion of the alkalinity in many oil-field water samples. In this study,

Table 5. Concentrations of dissolved organic and inorganic carbon, dissolved bicarbonate, del carbon-13 ($\delta^{13}\text{C}$) of dissolved inorganic carbon, carbon-14 (^{14}C), and dissolved aliphatic acids for samples from wells in the Edwards aquifer saline-water zone, south-central Texas, July–September 1990

[Samples from hydrologically stagnant group shown in bold. mg/L, milligrams per liter; <, less than; —, no data]

Sequence number (fig. 7)	Well number	Dissolved organic carbon (mg/L)	Dissolved inorganic carbon (mg/L)	Dissolved bicarbonate (mg/L)	$\delta^{13}\text{C}$ (per mil)	^{14}C (percent modern carbon)	Dissolved aliphatic acids ¹ (mg/L)
1	AY-68-37-523	2.6	52	300	-10.3	1.3	<1
2	DX-68-23-616	1.8	62	310	-3.20	1.9	17
3	KX-67-26-9—	3.5	67	500	-2.30	.8	<1
4	KR-67-52-6—	14	51	330	2.60	(2)	23
5	ZX-69-61-526	4.2	44	240	—	3.4	<1
6	AL-78-12-1—	21	53	420	.90	(2)	49
7	BU-67-19-4—	16	120	860	-4.80	1.0	<1
8	LR-67-01-812	5.7	77	480	-1.80	.5	11
10	AL-78-15-6—	14	55	220	-5.00	(2)	<5
11	PZ-67-58-6—	12	48	290	1.20	.7	19
12	YP-69-59-101	1.9	49	220	—	.6	<5
13	PZ-67-57-9—	13	41	260	-8.80	1.1	9
14	KX-67-26-3—	9.5	96	530	-11.7	(2)	<5
15	BU-67-19-1—	25	98	610	2.20	.2	12
16	PZ-67-58-7—	36	27	170	2.20	—	<5
17	AY-68-45-901	1.4	54	290	-3.20	(2)	—

¹ Analyses of aliphatic acids (acetic, propionic, isobutyric, n-butyric, and n-valeric) by Buck Henderson, Lower Colorado River Authority Environmental Laboratory, Austin, Tex. A gas chromatograph was used with flame ionization detector. Only acetic acid was detected in quantifiable amounts, except for well sample 16, which contained 1 mg/L propionic acid and 2 mg/L n-valeric acid.

² Below reporting level.

the aliphatic-acid anions are not a substantial proportion of the total alkalinity (table 5). Of the aliphatic-acid anions analyzed for, only acetic acid was detected consistently and in small concentrations relative to dissolved organic carbon and dissolved inorganic carbon concentrations determined in this study and to aliphatic acids determined in other studies (Gautier and others, 1985).

The sample from well AL-78-12-1— has the greatest amount of acetic acid (49 mg/L, or 0.81 anionic milliequivalents) (table 5). Most of the alkalinity (acid-neutralizing capacity) of the sample is from bicarbonate (6.9 milliequivalents). If the anionic milliequivalents

are assumed to be equivalent to the acid-neutralizing capacity, then the acetic-acid alkalinity is 11 percent of the total alkalinity of the sample. Bicarbonate alkalinity dominates the total alkalinity of this sample. The aliphatic-acid anion concentrations (all or mostly acetic acid, table 5) are much smaller in all other samples. Therefore, the alkalinity of the 16 samples collected for this study predominantly comprises bicarbonate, and the TP-file bicarbonate concentrations approximate the total alkalinity for those samples.

The reason for the relatively small concentrations of aliphatic acids compared to concentrations reported by Gautier and others (1985) is not clear. Most oil and

Table 6. Concentrations of selected dissolved gases for samples from wells in the Edwards aquifer saline-water zone, south-central Texas, July–September 1990

[Samples from hydrologically stagnant group shown in bold. In milligrams per liter at 22.5 degrees Celsius and atmospheric pressure. nd, not detected; —, no data]

Sequence number (fig. 7)	Well number	Nitrogen	Oxygen	Argon	Carbon dioxide	Ethane	Methane	Hydrogen sulfide
1	AY-68-37-523	23	nd	0.81	45	0.21	0.09	21
2	DX-68-23-616	25	nd	.08	30	nd	.04	nd
3	KX-67-26-9—	3.3	.76	.10	120	.82	4.2	260
4	KR-67-52-6—	.89	.06	.05	140	.53	2.0	140
5	ZX-69-61-526	—	—	—	—	—	—	—
¹ 6	AL-78-12-1—	—	—	—	300	.20	1.4	680
7	BU-67-19-4—	3.0	nd	.15	190	nd	6.8	240
8	LR-67-01-812	26	.19	.83	100	nd	.34	100
10	AL-78-15-6—	.35	.04	.05	320	.07	1.0	590
11	PZ-67-58-6—	—	—	—	—	—	—	—
12	YP-69-59-101	—	—	—	—	—	—	—
¹ 13	PZ-67-57-9—	—	—	—	100	.30	3.0	25
14	KX-67-26-3—	21	nd	.08	210	4.2	11	580
15	BU-67-19-1—	1.0	.07	<.01	150	.20	24	160
² 16	PZ-67-58-7—	52	5.2	.51	59	1.8	6.4	170
17	AY-68-45-901	20	—	.45	45	nd	.41	40

¹ Gas tube might have leaked. Carbon dioxide, methane, and hydrogen sulfide results are only qualitative.

² Concentrations listed are suspect.

gas fields in the Edwards aquifer saline-water zone are isolated because they formed where faults or other geologic structures created a zone of relative stagnation in the regional fluid flow sufficient to capture the buoyant hydrocarbon phase. Because of the small solubility of the hydrocarbons and the relative isolation of the hydrocarbon fields from ground-water flow, water along any given flowpath would most likely have little contact with hydrocarbons; thus, conditions are not favorable for hydrocarbon dissolution. The liquid petroleum most likely remains in a separate immiscible phase, and only small amounts dissolve in the brine.

Other dissolved carbon compounds probably constitute the dissolved organic carbon. Aside from gases, aliphatic-acid anions represent the most water-soluble compounds detected in substantial amounts in petroleum. Because of the high ratio of water to hydrocarbon in hydrocarbon production wells (Hendy, 1957; Cook,

1979), these small concentrations of dissolved organic compounds are representative of the Edwards aquifer brine.

Stable Isotopes

The $\delta^{13}\text{C}$ of inorganic carbon data in figure 13 and table 5 indicate multiple sources of dissolved inorganic carbon. This is consistent with the sulfur data because the sulfur-reducing and sulfur-oxidizing bacteria both require a carbon substrate. Additional $\delta^{13}\text{C}$ data of selected hydrocarbons reported by L.S. Land (Department of Geology, University of Texas at Austin, written commun., 1991) also indicate substantial bacterial activity.

The concentrations of several dissolved gases that contain carbon—carbon dioxide, ethane, and methane—are listed in table 6. Carbon dioxide is a

Table 7. Concentrations of minor dissolved ions for samples from wells in the Edwards aquifer saline-water zone, south-central Texas, July–September 1990

[Samples from hydrologically stagnant group shown in bold. In milligrams per liter]

Sequence number (fig. 7)	Well number	Boron	Bromide	Iodide	Iron	Lithium	Strontium
1	AY-68-37-523	1.7	4.3	0.25	0.23	0.86	12
2	DX-68-23-616	.81	2.4	.11	.03	.31	15
3	KX-67-26-9—	15	82	4.1	.20	7.7	45
4	KR-67-52-6—	250	420	65	1.3	120	1,700
5	ZX-69-61-526	.65	2.1	.16	.10	.40	14
6	AL-78-12-1—	220	820	45	2.2	190	910
7	BU-67-19-4—	8.4	42	2.3	.09	3.8	40
8	LR-67-01-812	4.8	22	1.1	.07	2.2	17
10	AL-78-15-6—	330	810	44	3.0	290	¹ 2,600
11	PZ-67-58-6—	240	560	49	1.7	120	¹ 2,100
12	YP-69-59-101	.34	.95	.072	.17	.16	11
13	PZ-67-57-9—	300	830	48	2.7	250	¹ 2,200
14	KX-67-26-3—	16	80	4.4	.20	7.6	42
15	BU-67-19-1—	9.3	42	2.1	.12	3.9	35
16	PZ-67-58-7—	270	820	45	2.9	200	¹ 1,800
17	AY-68-45-901	1.5	5.3	0.32	.05	.96	12

¹ Analysis by L.S. Land (Department of Geology, University of Texas at Austin).

component of dissolved inorganic carbon and is relatively soluble in water. Decarboxylation of petroleum organic matter is thought to be the origin of much of the carbon dioxide in oil-field brines (Gautier and others, 1985). Methane is extremely soluble in water, and all of the concentrations listed in table 6 are well below the saturation index for methane in water for the temperatures and pressures in the aquifer (Hanor, 1987b). Decarboxylation of aliphatic-acid anions is considered to be an important source for methane (natural gas) (Gautier and others, 1985). The estimated temperatures for the hydrologically stagnant samples probably are too high for microbial processes; however, the decarboxylation reactions might occur by thermocatalysis (Gautier and others, 1985). The temperatures of transition-group samples generally are less than

80 °C, the upper limit for substantial bacterial metabolism (Gautier and others, 1985), so bacteria probably are important to the geochemistry of the zone. Jorgensen and others (1992) indicate that sulfate-reduction microbial activity might occur at temperatures higher than 100 °C.

Other Dissolved Species

Dissolved sodium likely is from the same source as the dissolved chloride because carbonate rocks generally do not contain substantial amounts of sodium. Other major sources of dissolved sodium in the Edwards aquifer saline-water zone, such as ion exchange, are mineralogically or hydrologically unlikely. The concentrations of minor dissolved ions are listed in table 7.

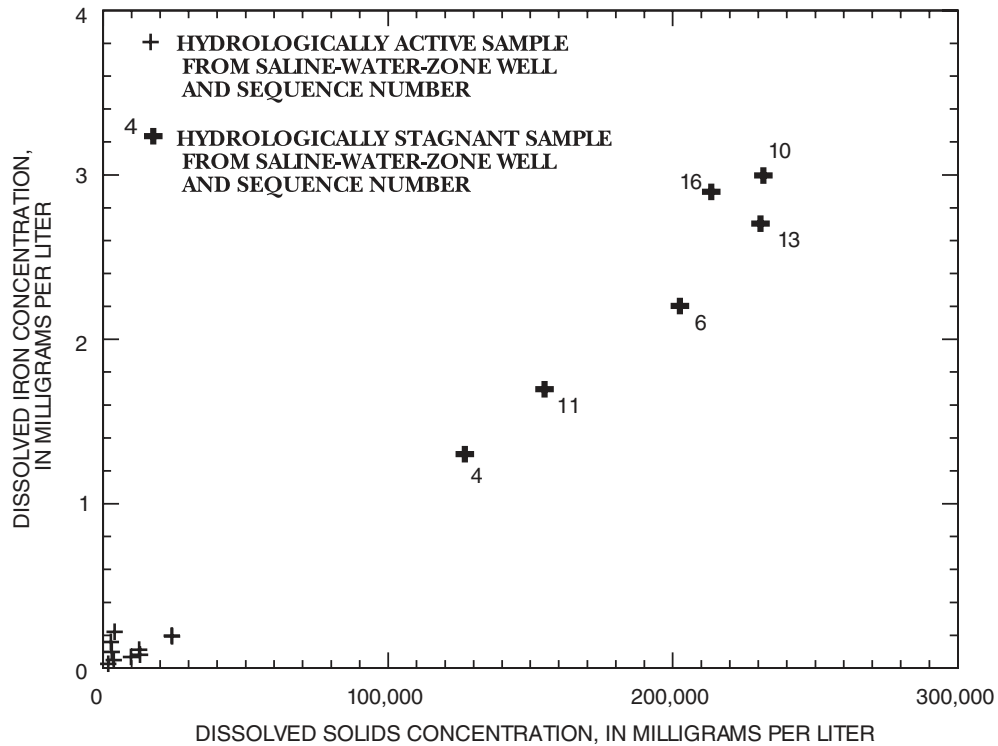


Figure 14. Relation between dissolved iron and dissolved solids concentrations in ground-water samples from the Edwards aquifer saline-water zone, south-central Texas

The relation between dissolved iron and dissolved solids concentrations is shown in figure 14. The reduced conditions of the saline water, inferred from the presence of hydrocarbons and hydrogen sulfide, indicate that the predominant dissolved iron species is ferrous iron, possibly in the form of a metal-organic complex. The increasing iron concentrations with increasing dissolved solids concentrations indicate that the amount of dissolved iron, although relatively small throughout the saline-water zone, is mostly a function of the ionic strength (as measured by dissolved solids concentration) and solubility limit of iron sulfide minerals. The thermochemical activity of ferrous iron in solution decreases with increasing dissolved solids, thereby allowing more dissolved ferrous iron to be in solution at larger dissolved solids concentrations. Substantial concentrations of hydrogen sulfide (table 6) indicate that dissolved sulfide is present in excess of what is required to maintain the iron sulfide mineral/aqueous-iron equilibrium distribution. The SIs of an iron sulfide mineral, pyrrhotite, are listed in table 3. Although it is not possible for SI alone to predict the mineral phases

that might precipitate from solution, the relative saturation state of the iron minerals indicates the relative stability of the iron sulfide minerals and the electrochemical environment in the saline-water zone.

The relation between dissolved potassium concentration and dissolved solids concentration in well-water samples is shown in figure 15. The potassium concentration is nonlinearly related to the dissolved solids concentration. Compared to the relation between dissolved iron and dissolved solids concentrations, the potassium concentration increases much more rapidly with ionic strength (as measured by dissolved solids) than does iron. The source of dissolved potassium could be (1) limestone or evaporite from the Edwards matrix, or (2) the Jurassic salts beneath the Edwards aquifer. The nonlinearity might be caused by increasing solubility with temperature. Land and Prezbindowski (1981) concluded that the potassium in the Edwards aquifer saline-water zone came from allochthonous brines that had passed through thick sections of clastic sediments. According to this hypothesis, the fluid passing through the clastic sediments gained dissolved potassium and

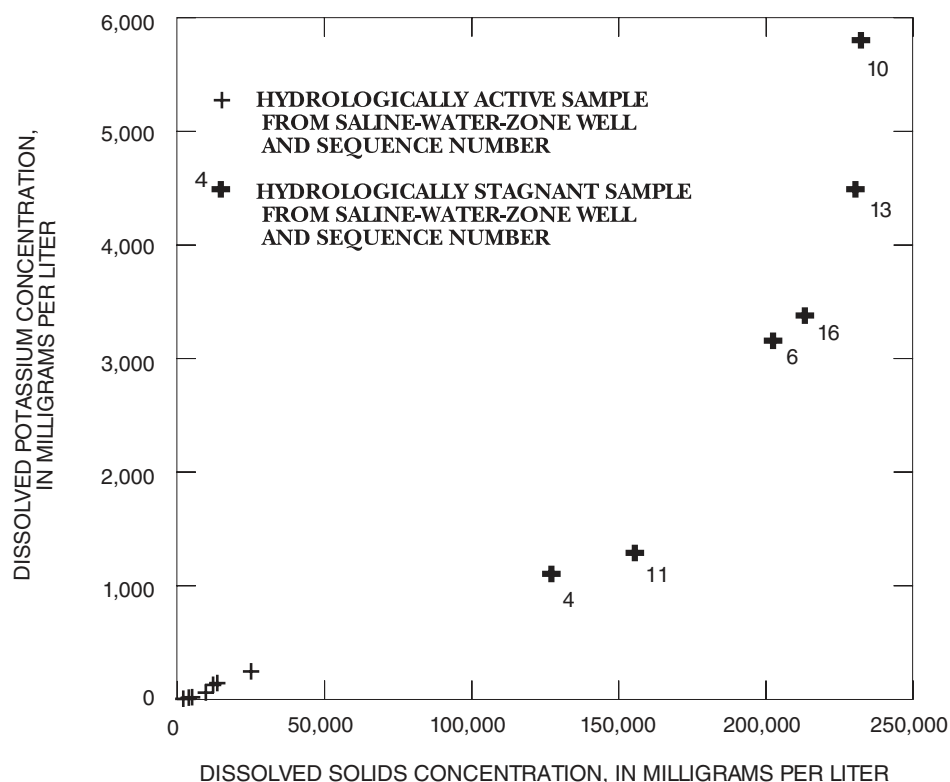


Figure 15. Relation between dissolved potassium and dissolved solids concentrations in ground-water samples from the Edwards aquifer saline-water zone, south-central Texas.

lost dissolved sodium by albitization—the process of converting potassic (or calcic) plagioclase to sodic plagioclase. This source of potassium is hydrologically unlikely given the geometry and stratigraphy of the Gulf Coast Basin (Wesselman, 1983). The clastic sediments (Cenozoic deposits) that contain plagioclase minerals are hundreds of meters stratigraphically above the Cretaceous sediments, and the intervening limestone, dolostone, and shale are virtually impermeable.

Other Isotopes

Stable Isotopes of Hydrogen and Oxygen

Stable-isotope ratios of hydrogen and oxygen (δD and $\delta^{18}O$) from 15 of the 16 well-water samples are listed in table 8. Meteoric water is defined as having δD and $\delta^{18}O$ that plot on or near the global meteoric water line, a relation developed by Craig (1961) to define the typical range of δD and $\delta^{18}O$ in precipitation (fig. 16). Depletion or enrichment of hydrogen and oxygen stable-isotope ratios refers to the relative amount of the heavier of the two isotopes as compared to the ratio in

Standard Mean Ocean Water (SMOW) (Yurtsever and Gat, 1981). In SMOW, by definition, $\delta D = \delta^{18}O = 0.0$.

The δD and $\delta^{18}O$ values separate the samples into two major groups: (1) hydrologically active samples from 9 shallow saline-water-zone wells with relatively small interwell variation; and (2) hydrologically stagnant samples from 6 deep brine wells that are enriched in deuterium and ^{18}O and have relatively large interwell variation. The hydrologically active group of samples, all of which are from wells less than 40 km from the downdip limit of freshwater, indicate meteoric water (fig. 16). The different δD and $\delta^{18}O$ of the hydrologically stagnant group of samples define a chemically distinct zone, regardless of the ultimate source of the water.

The stable-isotope content of the hydrologically active samples would not plot on the global meteoric water line if brine from a nonmeteoric recharge source (allochthonous) was mixing with Edwards aquifer water in the saline-water zone. Furthermore, a systematic variation (data transitional between the hydrologically active group and the hydrologically stagnant group) would be expected in the isotopic content among

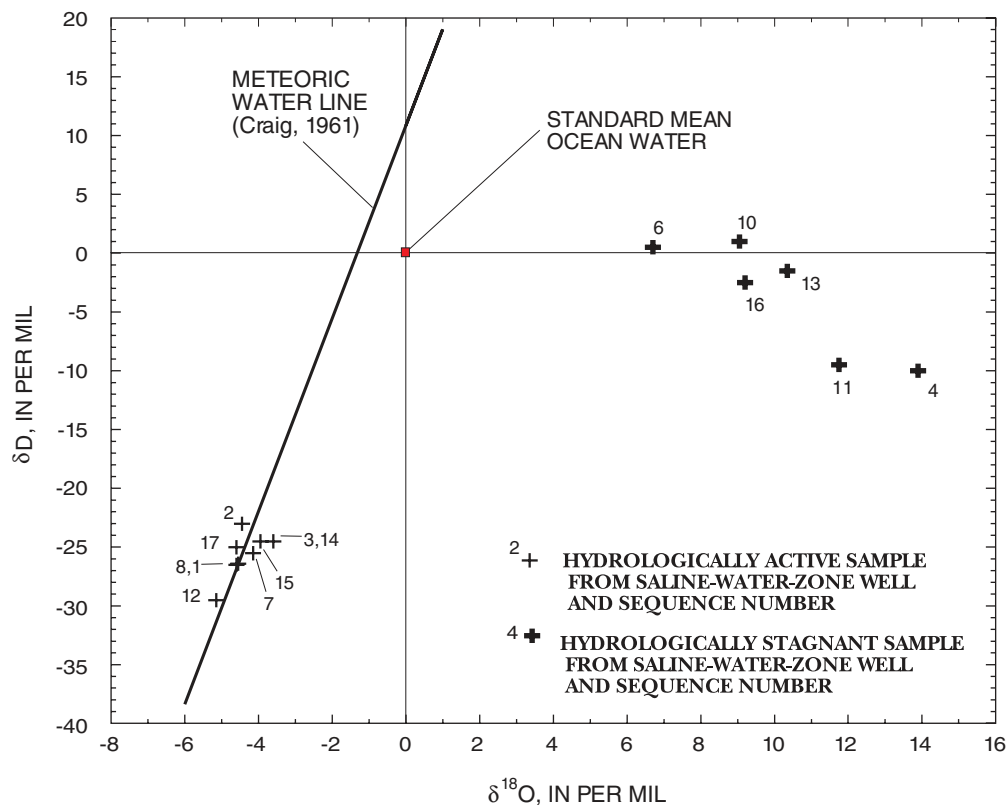


Figure 16. Relation between del deuterium (δD) and del oxygen-18 ($\delta^{18}\text{O}$) in ground-water samples from the Edwards aquifer saline-water-zone, south-central Texas.

samples caused by the varying amounts of allochthonous brine in the samples. None of the samples have intermediate δD and $\delta^{18}\text{O}$ that would indicate mixing between the meteoric water and another type—geothermal or otherwise. The fact that none of the 15 samples in figure 16 displays a mixed active/stagnant composition supports the assumption that little or no mixing is occurring between the two saline-water zones—a shallow, meteoric saline-water zone and a deep, stagnant saline-water zone.

The $\delta^{18}\text{O}$ of the calcite in the saline-water zone reported by Prezbindowski (1981) compared to $\delta^{18}\text{O}$ of the water samples are consistent with the concept that the shallow saline-water zone is meteoric, that it is open with respect to water, and that the isotope composition of the water is not in equilibrium with the minerals of the aquifer matrix. The deeper zone of higher salinity is separate and distinct in character, and the isotope composition of the water is in equilibrium with the aquifer-matrix minerals at the estimated in-place temperatures. The stagnant area is either a closed marine or a closed meteoric system or a combination of the closed systems.

Stable Isotopes of Strontium and Boron

The relation between the ratio of $^{87}\text{Sr}/^{86}\text{Sr}$ of dissolved strontium and dissolved strontium is shown in figure 17. The water-sample data fall into two distinct groups—the shallow, active, meteoric-water group and the deeper, stagnant, more saline water group. The data in figure 17 indicate only a vaguely positive relation between $^{87}\text{Sr}/^{86}\text{Sr}$ and dissolved strontium. Dissolved strontium concentration is uniform in samples from the hydrologically active group but highly variable in the samples from the hydrologically stagnant group. In contrast, $^{87}\text{Sr}/^{86}\text{Sr}$ varies widely in samples from the hydrologically active group but is uniform in samples from the hydrologically stagnant group, excluding sample 4. The relation between $^{87}\text{Sr}/^{86}\text{Sr}$ and dissolved strontium indicates a clear distinction between the two groups of well samples, a distinction previously defined with reference to other chemical data. The group of stagnant, more saline samples had much larger dissolved strontium concentration and a slightly higher

Table 8. Stable-isotope ratios of selected dissolved species for samples from wells in the Edwards aquifer saline-water zone, south-central Texas, July–September 1990

[Samples from hydrologically stagnant group shown in bold. Column headings defined on p. v. Units are per mil except for $^{87}\text{Sr}/^{86}\text{Sr}$, which is dimensionless. —, no data]

Sequence number (fig. 7)	Well number	$\delta^{34}\text{S}$, sulfate	$\delta^{34}\text{S}$, sulfide	δD	$\delta^{18}\text{O}$	$^{87}\text{Sr}/^{86}\text{Sr}^1$	$\delta^{11}\text{B}^1$
1	AY-68-37-523	21.5	-14.6	-26.5	-4.60	0.7081	21
2	DX-68-23-616	23.5	-16.9	-23.0	-4.45	.7082	15
3	KX-67-26-9—	35.5	4.1	-24.5	-3.60	.7088	23
4	KR-67-52-6—	—	12.5	-10.0	13.9	.7084	16
5	ZX-69-61-526	20.5	-16.9	—	—	.7078	29
6	AL-78-12-1—	30.4	14.6	0.5	6.70	.7094	20
7	BU-67-19-4—	37.5	10.2	-25.5	-4.15	.7082	28
8	LR-67-01-812	24.0	-9.6	-26.4	-4.55	.7084	25
10	AL-78-15-6—	32.3	15.7	1.0	9.05	.7094	16
11	PZ-67-58-6—	32.0	8.2	-9.5	11.8	.7096	18
12	YP-69-59-101	20.9	-3.4	-29.5	-5.15	.7084	21
13	PZ-67-57-9—	30.0	16.3	-1.5	10.4	.7093	18
14	KX-67-26-3—	42.1	3.9	-24.5	-3.60	.7088	29
15	BU-67-19-1—	41.1	2.5	-24.5	-3.95	.7079	21
16	PZ-67-58-7—	36.1	14.2	-2.5	9.20	.7095	23
17	AY-68-45-901	21.4	-14.1	-25.0	-4.60	.7078	20

¹ Analysis by L.S. Land (Department of Geology, University of Texas at Austin).

ratio of $^{87}\text{Sr}/^{86}\text{Sr}$ than the hydrologically active samples (fig. 17).

Strontium-87 is formed by rubidium-87 (^{87}Rb) decay (radiogenic). Isotope composition of dissolved strontium might indicate sources for the dissolved strontium. Relatively large ratios (greater than about 0.7200) indicate a detrital or silicate source, including shale or sandstone with substantial amounts of silicates (Stueber and others, 1984). Burke and others (1982) determined that the average $^{87}\text{Sr}/^{86}\text{Sr}$ ratio in Jurassic seawater was 0.7070, that the average ratio in Cretaceous seawater ranged from 0.7071 to 0.7080, and that marine limestone reflects the seawater ratio at the time of deposition. Oetting and others (1994) reported that the $^{87}\text{Sr}/^{86}\text{Sr}$ ratios in carbonate rocks of the Edwards aquifer range from 0.7074 to 0.7076. All of the $^{87}\text{Sr}/^{86}\text{Sr}$ in the Edwards aquifer saline-water-zone

samples are greater than the $^{87}\text{Sr}/^{86}\text{Sr}$ determined in the aquifer rocks (Oetting and others, 1994). The $^{87}\text{Sr}/^{86}\text{Sr}$ of the stagnant-group samples was greater than the $^{87}\text{Sr}/^{86}\text{Sr}$ of the active-group samples but not large enough to indicate a large amount of radiogenic strontium resulting from silicate diagenesis.

Strontium commonly is included in solid solution in calcium-containing minerals because of the similarity in size and chemistry of calcium and strontium atoms. Dissolution of carbonate minerals would release strontium into solution that has a $^{87}\text{Sr}/^{86}\text{Sr}$ similar to that of the carbonate minerals. The data shown in figure 17 are consistent with the hypothesis of an allochthonous brine derived from silicate diagenesis as proposed by Land and Prezbindowski (1985); however, the silicate sediments (Tertiary clastic sediments) in the Texas Gulf Coast subsurface lie stratigraphically above

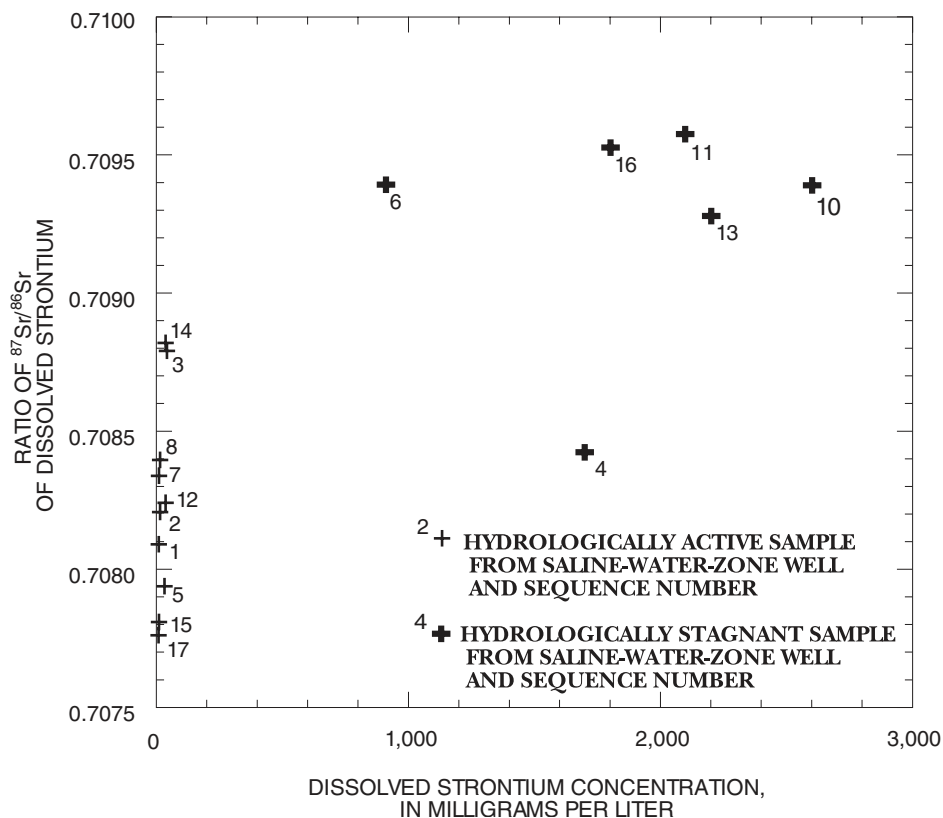


Figure 17. Relation between ratio of strontium-87/strontium-86 ($^{87}\text{Sr}/^{86}\text{Sr}$) of dissolved strontium and dissolved strontium concentration in ground-water samples from the Edwards aquifer saline-water zone, south-central Texas.

the Edwards aquifer, and hundreds of meters of Upper Cretaceous shale and limestone lie between the Tertiary clastic sediments and the Lower Cretaceous and Jurassic limestone and dolostone. Hanor (1987a) proposed that kilometer-scale vertical water convection could move silicate-influenced brines into the Edwards aquifer. Many studies of $^{87}\text{Sr}/^{86}\text{Sr}$ in waters or brines associated with carbonate rocks report that the fluid $^{87}\text{Sr}/^{86}\text{Sr}$ is greater than the rock $^{87}\text{Sr}/^{86}\text{Sr}$ (Stueber and others, 1984; Chaudhuri and others, 1987; Banner and Hanson, 1990).

Ranges of boron stable-isotope ratios in selected geological materials (Bassett, 1990) and 16 water samples from the Edwards aquifer saline-water zone are shown in figure 18. The range of $\delta^{11}\text{B}$ of dissolved boron in the Edwards aquifer ground-water samples is shown in figure 18 by two vertical dashed lines. The relation between $\delta^{11}\text{B}$ and dissolved solids concentration is shown in figure 19. The Edwards aquifer water

samples were analyzed by L.S. Land (Department of Geology, University of Texas at Austin).

Boron isotope data from the samples in the hydrologically active group and the hydrologically stagnant group of the Edwards aquifer are distinct (fig. 19). Except for sample 2, the $\delta^{11}\text{B}$ data from the hydrologically active group tend to plot in the upper range for Edwards aquifer samples, where they overlap the $\delta^{11}\text{B}$ range for marine evaporites (fig. 19). The $\delta^{11}\text{B}$ data from the hydrologically stagnant group of samples, except for samples 6 and 16, plot at the lower end of the range for Edwards aquifer samples, where they overlap the $\delta^{11}\text{B}$ range for geothermal water. These two graphs (figs. 18 and 19) corroborate the general distinction between the two major groups—the shallow, meteoric active samples having dissolved solids derived mostly from an evaporite source in the Edwards aquifer, and the deeper, more saline and geothermally affected stagnant samples of ambiguous or geothermal origin.

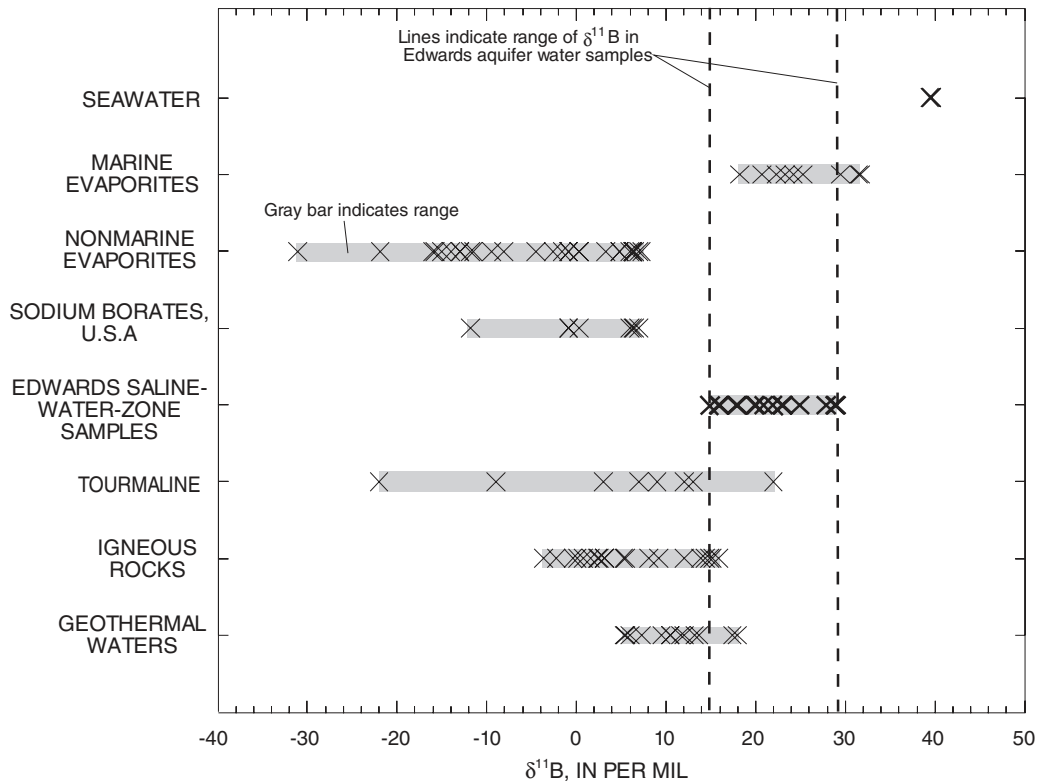


Figure 18. Ranges of del boron-11 ($\delta^{11}\text{B}$) of dissolved boron in selected natural materials and in water.

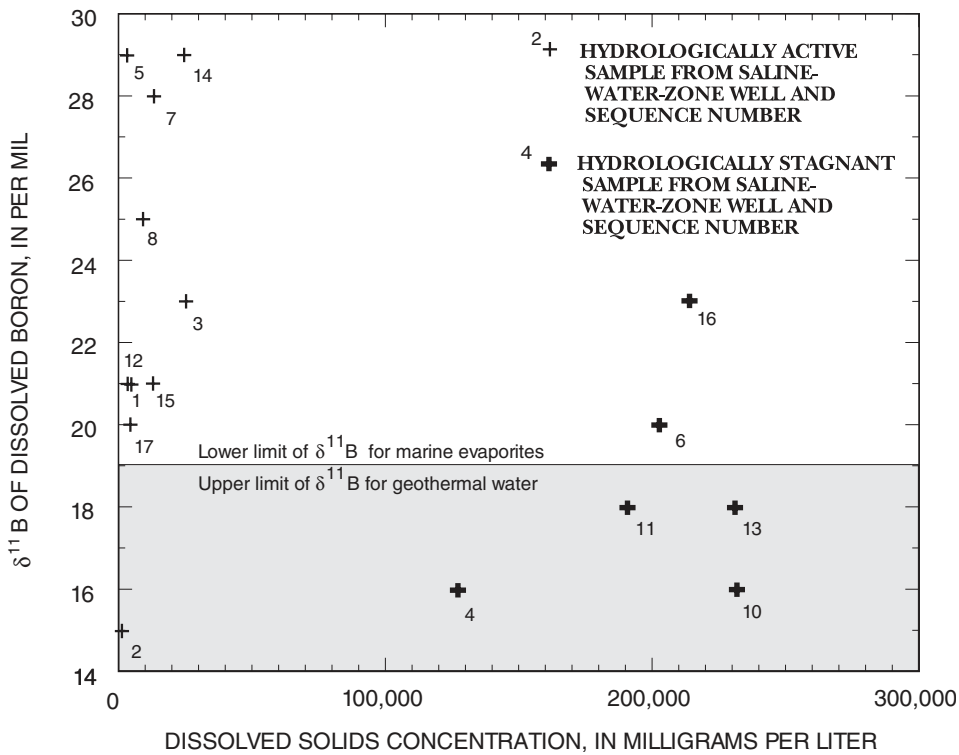


Figure 19. Relation between del boron-11 ($\delta^{11}\text{B}$) of dissolved boron and dissolved solids concentration in groundwater samples from the Edwards aquifer saline-water zone, south-central Texas.

Analysis of some Edwards aquifer saline-water-zone samples detected $\delta^{11}\text{B}$ as low as 11 per mil (L.S. Land, Department of Geology, University of Texas at Austin, written commun., 1992), well below the $\delta^{11}\text{B}$ range for marine evaporites.

Unstable Isotopes of Carbon and Chloride

All well-water samples, except sample 5 from well ZX-69-61-526, are nearly devoid of ^{14}C (table 5). This pattern of ^{14}C data might indicate that the amount of recent meteoric recharge (recharge occurring less than 10,000 years ago) to the saline-water zone generally is inconsequential, and that the average age of the water sampled is likely greater than 25,000 years. Alternatively, the carbonate mass transfer reactions between aqueous and solid phases might be of sufficient magnitude to completely dilute the dissolved inorganic carbon with dead (nonradioactive) carbon from the solid phase, thus inflating the computed age of the water.

Estimating the age of the ground-water samples from ^{14}C requires several assumptions, such as no mixing of water from separate flowpaths (fresh or saline) and no exchange of inorganic carbon from solution by precipitation or dilution of calcite or other carbonate minerals. These two assumptions are incompatible with the concept of dedolomitization as presented by Deike (1990) for the Edwards aquifer. Another required assumption is that no inorganic carbon is added to solution as a result of oxidation of hydrocarbons by either simple chemical oxidation or sulfate reduction by bacterial mediation or, in the transition zone, sulfide-oxidation dissolution of carbonate minerals. This assumption is incompatible with the sulfide-oxidation process proposed in this report ("Sulfur" subsection of "Dissolved Constituents" section) for the dissolved sulfate near the downdip limit of freshwater and is unlikely to be valid in any hydrocarbon-rich aquifer where sulfate-reducing bacteria are present.

Data for ^{14}C are available from several of the other wells in the San Antonio freshwater/saline-water transect. The ^{14}C , in percent modern carbon, of samples from the San Antonio transect wells in January 1989 are 45.6 in well AY-68-37-526, 56.3 in well AY-68-37-527 (both freshwater-zone wells near the downdip limit of freshwater), 40.5 in well AY-68-37-524 (shallow freshwater well), and below detection limit in well AY-68-37-525 (deep well). Well AY-68-37-525 is only 15 m north of and less than 91 m deeper than well AY-68-37-524. The robustness of the downdip limit of

freshwater against freshwater/saline-water mixing is indicated by the occurrence of such sharply contrasting ^{14}C content within distinct adjacent zones in Edwards aquifer water and of similar inorganic carbon content. The freshwater is young (less than a few thousands of years old) compared to the nearby saline water across the downdip limit of freshwater. Alternatively, sulfide oxidation and (or) hydrocarbon oxidation could be occurring in the aquifer near well AY-68-37-525 at substantial rates. If so, the ^{14}C of the initial dissolved inorganic carbon would be subject to precipitation as calcite and (or) dilution by the dead inorganic carbon produced by the reactions. Ultimately, the percent modern carbon of the dissolved inorganic carbon would be substantially reduced by mechanisms other than radioactive decay, thereby rendering ^{14}C dating invalid.

^{36}Cl has a half-life of 301,000 years, making it suitable for dating ground water past the limit of ^{14}C (Bentley and others, 1986). The analyses for $^{36}\text{Cl}/\text{Cl}$ (table 9) were done to determine the applicability of chlorine dating to the saline-water zone. After entering the aquifer in recharge water, the ^{36}Cl decays as the water ages, and the ratio of ^{36}Cl to ^{35}Cl of dissolved chloride (the common stable isotope) decreases logarithmically by radioactive decay. The number of ^{36}Cl atoms per liter also decreases unless there is another source of ^{36}Cl in the aquifer. In the Edwards aquifer saline-water zone, the secular equilibrium $^{36}\text{Cl}/\text{Cl}$ (steady-state background ratio) from subsurface production of ^{36}Cl is large relative to the $^{36}\text{Cl}/\text{Cl}$ of the initial chloride source.

The secular equilibrium $^{36}\text{Cl}/\text{Cl}$ is a result of the production of ^{36}Cl from ^{35}Cl by thermalized neutrons. ^{35}Cl has a relatively large particle cross section for absorbing thermalized neutron radiation from light element (α, n) reactions. The α -particles originate from decay processes of uranium or other unstable nuclei (Bentley and others, 1986). The Tertiary sediments of the Texas Gulf Coast subsurface are an economic source of uranium ore. Uranium deposits, or the processes that create them, could be a cause of a high neutron flux in the Texas Gulf Coast deposits. The ^{36}Cl of the meteoric recharge is diluted by the chloride added and imprinted by the secular equilibrium production in the deep saline-water zone. Therefore, the radiochloride data cannot be used for age-dating samples from the stagnant regime. A plot of the relation between $^{36}\text{Cl}/\text{Cl}$ and number of ^{36}Cl atoms per liter is shown in figure 20. The plot shows that the number of ^{36}Cl atoms per liter does not decline but instead increases as the $^{36}\text{Cl}/\text{Cl}$

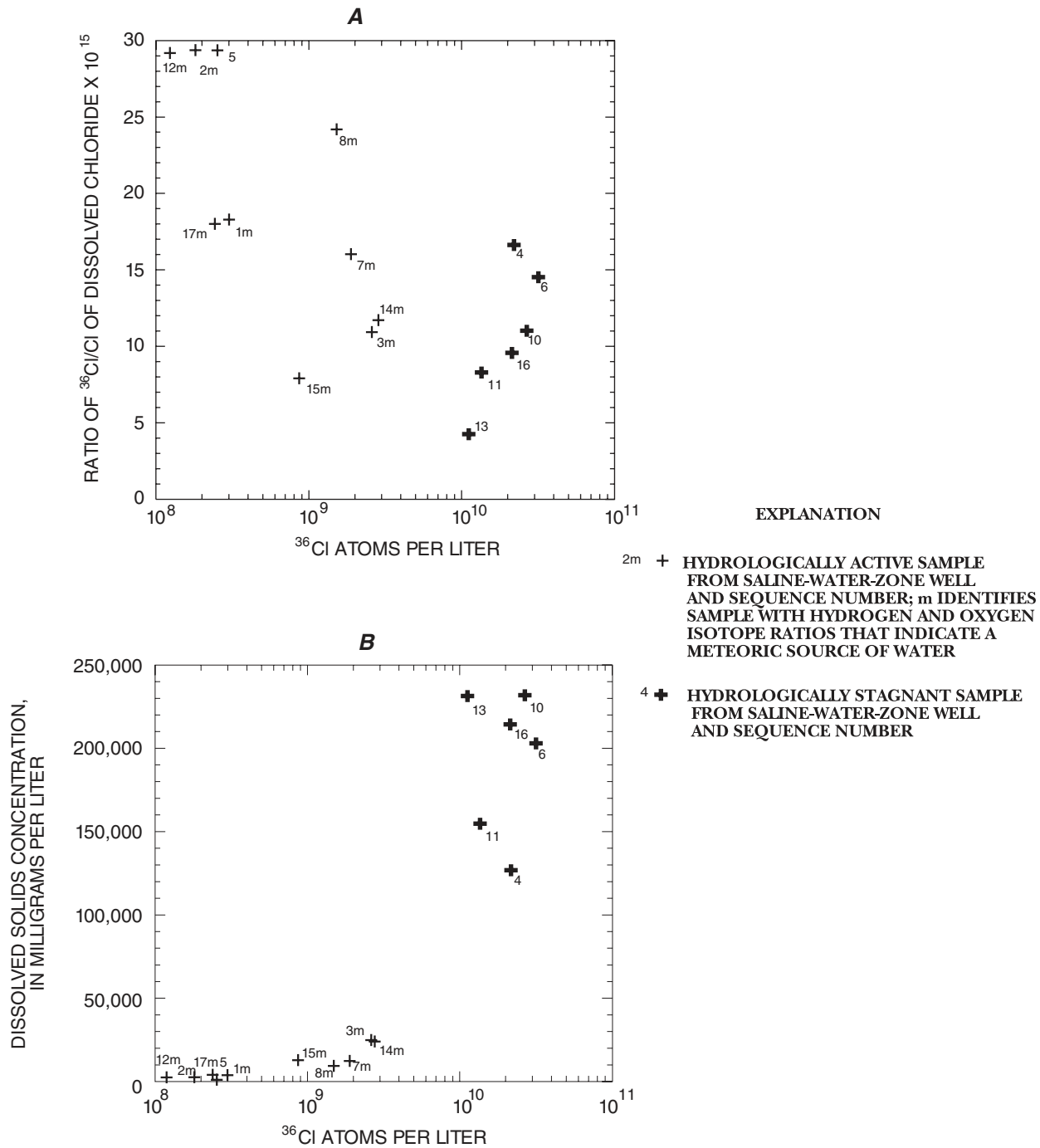


Figure 20. Relations between (A) ratio of chlorine-36/chlorine ($^{36}\text{Cl}/\text{Cl}$) of dissolved chloride and ^{36}Cl , and (B) dissolved solids concentration and ^{36}Cl in ground-water samples from the Edwards aquifer saline-water zone, south-central Texas.

decreases. The increase is slight for the water samples with meteoric stable-isotope ratios, but it is substantial for samples from the nonmeteoric, hydrologically stagnant group.

The $^{36}\text{Cl}/\text{Cl}$ of Cretaceous or older halite would be near zero, but the dissolved chloride would be at secular equilibrium for the aquifer, if sufficient residence time is assumed. The secular equilibrium ratio

Table 9. Ratio of chlorine-36 to chlorine ($^{36}\text{Cl}/\text{Cl}$), number of ^{36}Cl atoms per liter, and associated error for samples from wells in the Edwards aquifer saline-water zone, south-central Texas, July–September 1990

[Samples from hydrologically stagnant group shown in bold. All determinations by George Vourvopoulos (Western Kentucky University, written commun., 1992)]

Sequence number (fig. 7)	Well number	$^{36}\text{Cl}/\text{Cl} \pm$ standard deviation	^{36}Cl atoms per liter \pm standard deviation
1	AY-68-37-523	$18.3 \pm 2.6 \times 10^{-15}$	$30.2 \pm 4.3 \times 10^7$
2	DX-68-23-616	$29.4 \pm 3.3 \times 10^{-15}$	$25.5 \pm 2.9 \times 10^7$
3	KX-67-26-9—	$10.9 \pm 1.9 \times 10^{-15}$	$259 \pm 45 \times 10^7$
4	KR-67-52-6—	$16.7 \pm 2.7 \times 10^{-15}$	$2,160 \pm 349 \times 10^7$
5	ZX-69-61-526	$29.4 \pm 3.3 \times 10^{-15}$	$18.2 \pm 2.0 \times 10^7$
6	AL-78-12-1—	$14.6 \pm 2.4 \times 10^{-15}$	$3,100 \pm 510 \times 10^7$
7	BU-67-19-4—	$16.1 \pm 2.8 \times 10^{-15}$	$187 \pm 32 \times 10^7$
8	LR-67-01-812	$24.2 \pm 3.5 \times 10^{-15}$	$150 \pm 21 \times 10^7$
10	AL-78-15-6—	$11.1 \pm 2.0 \times 10^{-15}$	$2,640 \pm 476 \times 10^7$
11	PZ-67-58-6—	$8.3 \pm 1.9 \times 10^{-15}$	$1,340 \pm 307 \times 10^7$
12	YP-69-59-101	$29.2 \pm 3.4 \times 10^{-15}$	$12.2 \pm 1.4 \times 10^7$
13	PZ-67-57-9—	$4.3 \pm 1.6 \times 10^{-15}$	$1,020 \pm 381 \times 10^7$
14	KX-67-26-3—	$11.7 \pm 2.3 \times 10^{-15}$	$278 \pm 55 \times 10^7$
15	BU-67-19-1—	$7.9 \pm 2.0 \times 10^{-15}$	$90 \pm 23 \times 10^7$
16	PZ-67-58-7—	$9.6 \pm 2.2 \times 10^{-15}$	$2,120 \pm 486 \times 10^7$
17	AY-68-45-901	$18.0 \pm 2.7 \times 10^{-15}$	$24.2 \pm 3.6 \times 10^7$

of $^{36}\text{Cl}/\text{Cl}$ in the Edwards aquifer saline-water zone probably is no smaller than 4.3×10^{-15} (well 13, table 9), but likely is between 10×10^{-15} and 15×10^{-15} . Most of the $^{36}\text{Cl}/\text{Cl}$ values lie within a standard deviation of this range (table 9). Bentley and others (1986, p. 439) listed an average $^{36}\text{Cl}/\text{Cl}$ in brine ground water in limestone of $11.5 \pm 2.5 \times 10^{-15}$ for subsurface production level. The estimated initial $^{36}\text{Cl}/\text{Cl}$ of meteoric chloride for this area of south Texas is 30 to 40×10^{-15} (Bentley and others, 1986, p. 430). The radiochloride data for the hydrologically active group of samples (wells 1, 2, 3, 5, 7, 8, 12, 14, 15, 17) are within 2 standard deviations of either the likely range for secular equilibrium or the likely range of meteoric chloride. Therefore, the radiochloride data will not yield reliable estimates of age for samples in the hydrologically active group.

SUMMARY AND CONCLUSIONS

The Edwards aquifer supplies drinking water for more than 1 million people in south-central Texas. The saline-water zone of the Edwards aquifer extends from the downdip limit of freshwater to the southern and eastern edge of the Stuart City Formation. Water samples from 16 wells in the Edwards aquifer saline-water zone were collected during July–September 1990 and analyzed for major and minor dissolved constituents, selected stable isotopes, and radioisotopes. These data, supplemental data from an extensive water-quality data base, and data from other previous studies were interpreted to clarify the understanding of the saline-water-zone geochemistry.

Estimated in-place temperatures for the samples collected indicate an increase with depth and (or) distance from the downdip limit of freshwater. Water samples for pH indicate a decrease with increasing distance from the downdip limit of freshwater, but the decrease is caused partly by the increase in temperature. Dissolved major ions and dissolved solids concentrations all indicate a relatively monotonic increase in salinity from updip to downdip. The alkalinity of the water samples is predominantly bicarbonate because the low-molecular weight aliphatic-acid anion concentrations are small relative to the bicarbonate concentrations. The dissolved organic carbon concentrations also are lower than expected for an aquifer with economic amounts of oil and gas hydrocarbons.

Most of the isotope and geochemical data indicate at least two distinct hydrological and geochemical regimes in the saline-water zone of the Edwards aquifer. On the basis of hydrogen and oxygen isotopes and radiocarbon data, the shallower updip regime is predominantly meteoric water that has been recharged probably from the freshwater zone within recent geologic time (less than tens of thousands of years). Also, on the basis of hydrogen and oxygen isotope data, water in the hydrologically stagnant regime (downdip) has been thermally altered in reactions with the carbonate rocks of the zone. The deeper water probably is much older than water in the shallow zone and is nearly stagnant relative to that in the shallow zone. Almost all the data fit the concept of two regimes.

The geochemical distinction between the two groups of samples implies a hydrologic compartmentalization. The hydrogen and oxygen isotope ratios indicate that no mixing occurs between the two geochemical zones; therefore, the flowpaths of the two zones must be separated either by contrasts in permeability or by internal flow boundaries. Flow-barrier faults, similar to those in the freshwater zone, would create this kind of separation. Horizontal flow would be diverted parallel to the length of the fault. On the basis of the δD and $\delta^{18}O$ data, the flow of a deeper calcium-rich allochthonous brine up or down faults into the hydrologically active regime of the Edwards aquifer is unlikely. However, if hydraulic connection exists among deep aquifers in the Gulf Coast subsurface and if this connection is mediated by faults, then the withdrawal of fluids and concomitant pressure drop could cause or increase the movement of allochthonous fluid into the Edwards aquifer.

The geochemical grouping observed in the well-water data from well samples in the saline-water zone indicates that the zone is hydrologically compartmentalized, in part because of faults that function as barriers to downdip flow of recharge water. These fault barriers also probably impede updip flow. Flow compartmentalization and the resulting disparity in geochemistry between the two regimes indicate that updip movement of substantial amounts of saline water toward the freshwater zone is unlikely.

REFERENCES

- American Public Health Association and others, 1989, Standard methods for the examination of water and wastewater (17th ed.): Washington, D.C., American Public Health Association, 1,467 p.
- Banner, J.L., and Hanson, G.N., 1990, Calculation of simultaneous isotopic and trace element variations during water-rock interaction with applications to carbonate diagenesis: *Geochimica et Cosmochimica Acta*, v. 54, p. 3,123–3,137.
- Bassett, R.L., 1990, A critical evaluation of the available measurements for the stable isotopes of boron: *Applied Geochemistry*, v. 5, p. 541–554.
- Bebout, D.G., and Loucks, R.G., 1974, Stuart City trend Lower Cretaceous, south Texas, a carbonate shelf-margin model for hydrocarbon exploration: Austin, University of Texas, Bureau of Economic Geology Report of Investigations 78, 80 p.
- Beckman, J.D., and Williamson, A.K., 1990, Salt-dome locations in the Gulf Coastal Plain, south-central United States: U.S. Geological Survey Water-Resources Investigations Report 90–4060, 44 p.
- Bentley, H.W., Phillips, F.M., and Davis, S.N., 1986, ^{36}Cl in the terrestrial environment, in Fritz, Peter, and Fontes, J.C., eds., 1986, Handbook of environmental isotope geochemistry, v. 2, The terrestrial environment, B: Amsterdam, Elsevier, p. 427–480.
- Bodine, M.W., Jr., and Jones, B.F., 1986, The salt norm—A quantitative chemical-mineralogical characterization of natural waters: U.S. Geological Survey Water-Resources Investigations Report 86–4086, 130 p.
- Brown, D.S., Gilhousen, J.R., and Nalley, G.M., 1991, Compilation of hydrologic data for the Edwards aquifer, San Antonio area, Texas, 1990, with 1934–90 summary: San Antonio, Edwards Underground Water District Bulletin 50, 169 p.
- Brown, D.S., Petri, B.L., and Nalley, G.M., 1992, Compilation of hydrologic data for the Edwards aquifer, San Antonio area, Texas, 1991, with 1934–91 summary: San Antonio, Edwards Underground Water District Bulletin 51, 169 p.

- Burke, W.H., Denison, R.E., Hetherington, E.A., Koepnick, R.B., Nelson, H.F., and Otto, J.B., 1982, Variation of seawater $^{87}\text{Sr}/^{86}\text{Sr}$ throughout Phanerozoic time: *Geology*, v. 10, p. 516–519.
- Carothers, W.W., and Kharaka, Y.K., 1978a, Aliphatic acid anions in oil-field waters—Implications for origin of natural gas: *American Association of Petroleum Geologists Bulletin*, v. 62, p. 2,441–2,453.
- _____, 1978b, Stable carbon isotopes in oil-field waters and the origin of CO_2 : *Geochimica et Cosmochimica Acta*, v. 44, p. 323–333.
- Chaudhuri, S., Broedel, V., and Clauer, N., 1987, Strontium isotope evolution of oil-field waters from carbonate reservoir rocks in Bindley field, central Kansas, U.S.A.: *Geochimica et Cosmochimica Acta*, v. 51, p. 45–53.
- Claassen, H.C., 1982, Guidelines and techniques for obtaining water samples that accurately represent the water chemistry of an aquifer: U.S. Geological Survey Open-File Report 82–1024, 49 p.
- Claypool, G.E., Holser, W.T., Kaplan, I.R., Sakai, Hitoshi, and Zak, Israel, 1980, The age curves of sulfur and oxygen isotopes in marine sulfate and their mutual interpretation: *Chemical Geology*, v. 28, p. 199–260.
- Clement, T.J., and Sharp, J.M., Jr., 1988, Hydrochemical facies in the bad-water zone of the Edwards aquifer, central Texas, *in* Ground water geochemistry, National Water Well Association Conference, Proceedings: Dublin, Ohio, p. 127–149.
- Cook, T.D., 1979, Exploration history of South Texas Lower Cretaceous carbonate platform: *American Association of Petroleum Geologists Bulletin*, v. 63, no. 1, p. 32–49.
- Craig, Harmon, 1961, Isotopic variations in meteoric waters: *Science*, v. 133, no. 3465, p. 1,702–1,703.
- Dahlberg, E.C., 1982, Applied hydrodynamics in petroleum exploration: New York, Springer-Verlag, 161 p.
- Deike, R.G., 1990, Dolomite dissolution rates and possible Holocene dedolomitization of water-bearing units in the Edwards aquifer, south-central Texas: *Journal of Hydrology*, v. 112, no. 3/4, p. 335–373.
- Feely, H.W., and Kulp, J.L., 1957, Origin of Gulf Coast salt-dome sulphur deposits: *American Association of Petroleum Geologists Bulletin*, v. 41, no. 8, p. 1,802–1,853.
- Fisher, J.B., 1987, Distribution and occurrence of aliphatic acid anions in deep subsurface waters: *Geochimica et Cosmochimica Acta*, v. 51, p. 2,459–2,468.
- Fisher, W.L., and Rodda, P.U., 1969, Edwards Formation (Lower Cretaceous), Texas—Dolomitization in a carbonate platform system: *American Association of Petroleum Geologists Bulletin*, v. 53, no. 1, p. 55–72.
- Fishman, M.J., and Friedman, L.C., eds., 1989, Methods for determination of inorganic substances in water and fluvial sediments: U.S. Geological Survey Techniques of Water-Resources Investigations, book 5, chap. A1, 545 p.
- Garrels, R.M., and Christ, C.L., 1965, Solutions, minerals, and equilibria: San Francisco, Freeman, Cooper, and Co., 450 p.
- Gautier, D.L., Kharaka, Y.K., and Surdam, R.C., 1985, Relationship of organic matter and mineral diagenesis: Tulsa, Okla., Society of Economic Paleontologists and Mineralogists, Notes for short course 17, 279 p.
- Getzender, F.M., 1930, Geologic section of the Rio Grande embayment, Texas, and implied history: *American Association of Petroleum Geologists Bulletin*, v. 14, no. 11, p. 1,425–1,437.
- Groschen, G.E., 1994, Analysis of data from test-well sites along the downdip limit of freshwater in the Edwards aquifer, San Antonio, Texas, 1985–87: U.S. Geological Survey Water-Resources Investigations Report 93–4100, 92 p.
- Hach Co., 1989, DR 2000 spectrophotometer handbook: Loveland, Colo., 395 p.
- Hanor, J.S., 1979, The sedimentary genesis of hydrothermal fluids, *in* Barnes, H.L. ed., *Geochemistry of hydrothermal ore deposits*: New York, Wiley Interscience, p. 137–168.
- _____, 1987a, Kilometer-scale thermohaline overturn of pore fluid in the Louisiana Gulf Coast: *Nature*, v. 327, p. 501–503.
- _____, 1987b, Origin and migration of subsurface sedimentary brines: Tulsa, Okla., Society of Economic Paleontologists and Mineralogists, Notes for short course 21, 247 p.
- Hendy, W.J., 1957, Lower Cretaceous (Edwards) oil fields, Caldwell and Guadalupe Counties, Texas: *Gulf Coast Association of Geological Societies Transactions*, v. 7, p. 23–34.
- Hill, C.A., 1990, Sulfuric acid speleogenesis of Carlsbad Cavern and its relationship to hydrocarbons, Delaware Basin, New Mexico and Texas: *American Association of Petroleum Geologists Bulletin*, v. 74, no. 11, p. 1,685–1,694.
- Hobba, W.A., Jr., Chemerys, J.C., Fisher, D.W., and Pearson, F.J., Jr., 1977, Geochemical and hydrologic data for wells and springs in thermal-spring areas of the Appalachians: U.S. Geological Survey Water-Resources Investigations Report 77–25, 36 p.
- Jorgensen, B.B., Isaksen, M.F., and Jannasch, H.W., 1992, Bacterial sulfate reduction above 100 °C in deep-sea hydrothermal vent sediments: *Science*, v. 258, p. 1,756–1,757.
- Kharaka, Y.K., Gunter, W.D., Aggarwal, P.K., Perkins, E.H., and DeBraal, J.D., 1988, SOLMINEQ.88—A computer program for geochemical modeling of water-rock interactions: U.S. Geological Survey Water-Resources Investigations Report 88–4227, 420 p.
- Krouse, H.R., 1980, Sulfur isotopes in our environment, *in* Fritz, Peter, and Fontes, J.C., eds., *Handbook of*

- environmental isotope geochemistry, v. 1, The terrestrial environment, A: Amsterdam, Elsevier, p. 435–472.
- Land, L.S., and Prezbindowski, D.R., 1981, The origin and evolution of saline formation water, Lower Cretaceous carbonates, south-central Texas, U.S.A.: *Journal of Hydrology*, v. 54, p. 51–74.
- _____, 1985, Chemical constraints and origins of four groups of Gulf Coast reservoir fluids—Discussion: *American Association of Petroleum Geologists Bulletin*, v. 69, no. 1, p. 119–126.
- Lico, M.S., Kharaka, Y.K., Carothers, W.W., and Wright, V.A., 1982, Methods for collection and analysis of geopressured geothermal and oil field waters: U.S. Geological Survey Water-Supply Paper 2194, 21 p.
- Lozo, F.E., Jr., and Smith, C.I., 1964, Revision of Comanche Cretaceous stratigraphic nomenclature, southern Edwards Plateau, southwest Texas: *Gulf Coast Association of Geological Societies Transactions*, v. 14, p. 285–306.
- Lundegard, P.D., and Land, L.S., 1986, Carbon dioxide and organic acids—Their role in porosity enhancement and cementation, Paleogene of the Texas Gulf Coast, *in* Gautier, D.L., ed., *Roles of organic matter in sediment diagenesis—Based on a symposium: Tulsa, Okla., Society of Economic Paleontologists and Mineralogists Special Publication 38*, p. 129–146.
- Maclay, R.W., and Land, L.F., 1988, Simulation of flow in the Edwards aquifer, San Antonio region, Texas, and refinement of storage and flow concepts: U.S. Geological Survey Water-Supply Paper 2336–A, 48 p.
- Maclay, R.W., and Small, T.A., 1984, Carbonate geology and hydrology of the Edwards aquifer in the San Antonio area, Texas: U.S. Geological Survey Open-File Report 83–537, 72 p.
- Mench-Ellis, P.M., 1985, Diagenesis of the Lower Cretaceous Edwards Group in the Balcones fault zone area, south-central Texas: Austin, University of Texas, Ph.D. dissertation, 326 p.
- Moredock, D.F., and Van Sicle, D.C., 1964, Regional variations of hydrocarbons in the Edwards Limestone (Cretaceous) of south Texas: *Gulf Coast Association of Geological Societies Transactions*, v. 14, p. 253–261.
- Morrow, D.W., 1982, Diagenesis 1. Dolomite—Part 1, The chemistry of dolomitization and dolomite precipitation: *Geoscience Canada*, v. 9, no. 1, p. 5–13.
- Nalley, G.M., 1989, Compilation of hydrologic data for the Edwards aquifer, San Antonio area, Texas, 1988, with 1934–88 summary: *San Antonio, Edwards Underground Water District Bulletin 48*, 157 p.
- Nalley, G.M., and Thomas, M.W., 1990, Compilation of hydrologic data for the Edwards aquifer, San Antonio area, Texas, 1989, with 1934–89 summary: *San Antonio, Edwards Underground Water District Bulletin 49*, 155 p.
- Oetting, G.C., Banner, J.L., and Sharp, J.M., Jr., 1994, Regional geochemical and isotopic variations in badwaters of the Edwards aquifer, *in* Edwards aquifer field trip guidebook, Toxic Substances and the Hydrologic Sciences Conference, Austin, Tex., April 10–13, 1994: American Institute of Hydrology, p. 1–13.
- Pavlicek, D.L., Small, T.A., and Rettman, P.L., 1987, Hydrogeologic data from a study of the freshwater zone/salinewater zone interface in the Edwards aquifer, San Antonio region, Texas: U.S. Geological Survey Open-File Report 87–389, 108 p.
- Pearson, F.J., and Rightmire, C.T., 1980, Sulphur and oxygen isotopes in aqueous sulphur compounds, *in* Fritz, Peter, and Fontes, J.C., eds., *Handbook of environmental isotope geochemistry, v. 1, The terrestrial environment, A: Amsterdam, Elsevier*, p. 227–258.
- Perez, Roberto, 1986, Potential for updip movement of salinewater in the Edwards aquifer, San Antonio, Texas: U.S. Geological Survey Water-Resources Investigations Report 86–4032, 21 p.
- Pettijohn, R.A., 1986, Processing water-chemistry data of Gulf Coast aquifer systems, south-central United States, with summary of dissolved-solids concentrations and water types: U.S. Geological Survey Water-Resources Investigations Report 86–4186, 42 p.
- Plummer, L.N., Busby, J.F., Lee, R.W., and Hanshaw, B.B., 1990, Geochemical modeling of the Madison aquifer in parts of Montana, Wyoming, and South Dakota: *Water Resources Research*, v. 26, no. 9, p. 1,981–2,014.
- Poteet, Diane, Collier, Hughbert, and Maclay, R.W., 1992, Investigation of the fresh/saline-water interface in the Edwards aquifer in New Braunfels and San Marcos, Texas: San Antonio, Edwards Underground Water District Report 92–02, 171 p.
- Prezbindowski, D.R., 1981, Carbonate rock-water diagenesis, Lower Cretaceous, Stuart City trend, south Texas: Austin, University of Texas, Ph.D. dissertation, 236 p.
- _____, 1985, Burial cementation—Is it important? A case study, Stuart City trend, south central Texas, *in* Carbonate cements: Tulsa, Okla., Society of Economic Paleontologists and Mineralogists Special Publication 37, p. 241–264.
- Pritt, Jeffrey, and Jones, B.E., eds., 1990, 1990 National Water Quality Laboratory services catalog: U.S. Geological Survey Open-File Report 89–386 [variously paged].
- Puente, Celso, 1978, Method of estimating natural recharge to the Edwards aquifer in the San Antonio area, Texas: U.S. Geological Survey Water-Resources Investigations Report 78–10, 38 p.
- Rightmire, C.T., Pearson, F.J., Jr., Back, William, Rye, R.O., and Hanshaw, B.B., 1974, Distribution of sulfur isotopes in ground waters from the principal artesian aquifer of Florida and the Edwards aquifer of Texas, United States

- of America, *in* Isotope techniques: Groundwater Hydrology, v. 2, IAEA, p. 191–207.
- Rose, P.R., 1972, Edwards Group, surface and subsurface, central Texas: Austin, Tex., University of Texas, Bureau of Economic Geology Report of Investigations 74, 198 p.
- _____, 1984, Oil and gas occurrence in Lower Cretaceous rocks, Maverick Basin area, southwest Texas, *in* Smith, C.I., ed., 1984, Stratigraphy and structure of the Maverick Basin and Devils River trend, Lower Cretaceous, southwest Texas: South Texas Geological Society field trip 6, American Association of Petroleum Geologists convention, 1984, p. 27–40.
- Rye, R.O., Back, William, Hanshaw, B.B., Rightmire, C.T., and Pearson, F.J., Jr., 1981, The origin and isotopic composition of dissolved sulfide in groundwater from carbonate aquifers in Florida and Texas: *Geochimica et Cosmochimica Acta*, v. 45, no. 10, p. 1,941–1,950.
- Slagle, D.L., Ardis, A.F., and Slade, R.M., Jr., 1986, Recharge zone of the Edwards aquifer hydrologically associated with Barton Springs in the Austin area, Texas: U.S. Geological Survey Water-Resources Investigations Report 86–4062, 1 sheet, scale 1:24,000.
- Stueber, A.M., Pushkar, P., and Hetherington, E.A., 1984, A strontium isotopic study of Smackover brines and associated solids, southern Arkansas: *Geochimica et Cosmochimica Acta*, v. 48, p. 1,637–1,649.
- Taylor, R.E., 1975, Chemical analyses of ground water for saline-water resources studies in Texas Coastal Plain stored in National Data Storage and Retrieval System: U.S. Geological Survey Open-File Report 75–79, 669 p.
- Thatcher, L.L., Janzer, V.J., and Edwards, K.W., 1977, Methods for determination of radioactive substances in water and fluvial sediment: U.S. Geological Survey Techniques of Water-Resources Investigations, book 5, chap. A5, p. 17–22.
- Tucker, D.R., 1962, Subsurface Lower Cretaceous stratigraphy, central Texas, *in* Contributions to the geology of south Texas: San Antonio, South Texas Geological Society, p. 177–217.
- _____, 1967, Faults of south and central Texas: Gulf Coast Association of Geological Societies Transactions, v. 17, p. 144–147.
- University of Texas, Bureau of Economic Geology, 1974, Geologic atlas of Texas, Seguin sheet: Austin, University of Texas, Bureau of Economic Geology, scale 1:250,000. (Reprinted 1979.)
- _____, 1981a, Geologic atlas of Texas, Austin sheet: Austin, University of Texas, Bureau of Economic Geology, scale 1:250,000.
- _____, 1981b, Geologic atlas of Texas, Llano sheet: Austin, University of Texas, Bureau of Economic Geology, scale 1:250,000.
- _____, 1984, Geologic atlas of Texas, San Antonio sheet: Austin, University of Texas, Bureau of Economic Geology, scale 1:250,000.
- Wershaw, R.L., Fishman, M.J., Grabbe, R.R., and Lowe, L.E., eds., 1987, Methods for determination of organic substances in water and fluvial sediments: U.S. Geological Survey Techniques of Water Resources Investigations, book 5, chap. A3, 80 p.
- Wesselman, J.B., 1983, Structure, temperature, pressure and salinity of Cenozoic aquifers of south Texas: U.S. Geological Survey Hydrologic Investigations Atlas HA–645, 1 plate.
- William F. Guyton Associates, Inc., 1986, Drilling, construction, and testing of monitor wells for the Edwards aquifer bad-water line experiment: Consultant report to the San Antonio City Water Board. On file at U.S. Geological Survey, 435 Isom Rd., Suite 234, San Antonio, Texas 78216.
- Williamson, A.K., Grubb, H.F., and Weiss, J.S., 1990, Ground-water flow in the Gulf Coast aquifer systems, south-central United States—A preliminary analysis: U.S. Geological Survey Water-Resources Investigations Report 89–4071, 124 p.
- Winter, J.A., 1961, Fredericksburg and Washita strata (sub-surface Lower Cretaceous), southwest Texas: Austin, University of Texas, Ph.D. dissertation, 135 p.
- Wood, W.W., 1976, Guidelines for collection and field analysis of ground-water samples for selected unstable constituents: U.S. Geological Survey Techniques of Water-Resources Investigations, book 1, chap. D2, 24 p.
- Woodruff, C.M., Jr., and Foley, Duncan, 1985, Thermal regimes of the Balcones/Ouachita trend, central Texas: Gulf Coast Association of Geological Societies Transactions, v. 35, p. 287–292.
- Yurtsever, Yuri, and Gat, J.R., 1981, Atmospheric water, *in* Stable isotope hydrology—Deuterium and oxygen-18 in the water cycle: Vienna, International Atomic Energy Agency Technical Report Series, no. 210, p. 103–142.